
Effects of Gradation and Cohesion on Bridge Scour, Vol. 2. Experimental Study of Sediment Gradation and Flow Hydrograph Effects on Clear Water Scour Around Circular Piers

PUBLICATION NO. FHWA-RD-99-184

DECEMBER 1999

PB2000-103271



U.S. Department of Transportation

Federal Highway Administration

Research, Development, and Technology
Turner-Fairbank Highway Research Center
6300 Georgetown Pike
McLean, VA 22101-2296

REPRODUCED BY:
U.S. Department of Commerce
National Technical Information Service
Springfield, Virginia 22161



FOREWORD

This report is volume 2 of a six volume series describing detailed laboratory experiments conducted at Colorado State University for the Federal Highway Administration as part of a study entitled "Effects of Sediment Gradation and Cohesion on Bridge Scour". Volume 2 describes the effects of sediment gradation and flow hydrographs on local clear water pier scour. This six volume series will be distributed to NTIS only and will not be printed by FHWA. A separate summary report which describes the key results from the six volume series will be published by FHWA and distributed to the FHWA Division Offices.



T. Paul Teng, P.E.
Director, Office of Infrastructure
Research and Development

NOTICE

This document is disseminated under the sponsorship of the Department of Transportation in the interest of information exchange. The United States Government assumes no liability for the contents or use thereof. This report does not constitute a standard, specification, or regulation.

The United States Government does not endorse products or manufacturers. Trade and manufacturers names appear in this report only because they are considered essential to the object of the document.

PROTECTED UNDER INTERNATIONAL COPYRIGHT
ALL RIGHTS RESERVED
NATIONAL TECHNICAL INFORMATION SERVICE
U.S. DEPARTMENT OF COMMERCE

Reproduced from
best available copy.



1. Report No. FHWA-RD-99-184	2. PB2000-103271 	3. Recipient's Catalog No.	
4. Title and Subtitle EFFECTS OF GRADATION AND COHESION ON BRIDGE SCOUR Vol. 2. Experimental Study of Sediment Gradation and Flow Hydrograph Effects on Clear Water Scour Around Circular Piers		5. Report Date December 1999	
		6. Performing Organization Code	
7. Author(s) Albert Molinas and Hani M. Noshi		8. Performing Organization Report No.	
9. Performance Organization Name and Address Colorado State University Engineering Research Center Fort Collins, Colorado		10. Work Unit No. (TRAIS) NCP# 3D3C1-582	
		11. Contract or Grant No. DTFH61-91-C-00004	
12. Sponsoring Agency and Address Office of Engineering Research and Development Federal Highway Administration 6300 Georgetown Pike MxclLean, Va 22101		13. Type of Report and Period Covered Laboratory Final Report Jan 1991 - Jan 1996	
		14. Sponsoring Agency Code	
15. Supplementary Notes Contracting Officer's Technical Representative: J. Sterling Jones HNR-10			
16. Abstract <p>In the first part of this experimental study effects of sediment size gradation on clear-water pier scour was studied using four sand mixtures with median sediment sizes (D_{50}) of 0.76 mm, 1.8 mm, and 1.87 mm and with different gradation coefficients. Experiments were conducted in the two-foot-wide by sixty-foot-long experimental flume at the Engineering Research Center, Colorado State University using 2 in., 2.50 in. and 2.75 in. diameter (51, 64, and 70 mm) circular piers. A regression equation was derived to fit the experimental data specific to the particular pier and flow conditions used in the experiments. This equation shows that gradation effects are not constant through the entire range of flow conditions but vary with flow intensity.</p> <p>In the second part of the experimental study, effects of flow hydrograph is investigated by subjecting circular piers used in the first part to bursts of discharges of varying duration and rate of increase. It is found that up to 60 percent of ultimate scour could be attained in short duration events for rapidly increasing flow conditions. Results are expressed in the form of a regression expression using one of the test cases as the normalizing event.</p> <p>This publication is the second volume of a six volume series. The other volumes are as follows:</p> <p>Vol. 1. Effect of Sediment Gradation and Coarse Material Fraction on Clear Water Scour Around Bridge Piers</p> <p>Vol. 3. Abutment Scour for Nonuniform Mixtures</p> <p>Vol. 4. Experimental Study of Scour Around Circular Piers in Cohesive Soils</p> <p>Vol. 5. Effect of Cohesion on Bridge Abutment Scour</p> <p>Vol. 6. Abutment Scour in Uniform and Stratified Sand Mixtures</p>			
17. Key Words Bridge Scour, Pier Scour, Abutment Scour, Gradation, Coarse Sediment, Cohesion, Clay Scour		18. Distribution Statement No restrictions. This document is available to the public through the National Technical Information Service, Springfield, Va. 22161	
19. Security Classif. (of this report) Unclassified	20. Security Classif. (of this page) Unclassified	21. No. of Pages 89	22. Price

SI* (MODERN METRIC) CONVERSION FACTORS

APPROXIMATE CONVERSIONS FROM SI UNITS

Symbol	When You Know	Multiply By	To Find	Symbol	When You Know	Multiply By	To Find	Symbol
LENGTH								
in	inches	25.4	millimeters	mm	millimeters	0.039	inches	in
ft	feet	0.305	meters	m	meters	3.28	feet	ft
yd	yards	0.914	meters	m	meters	1.09	yards	yd
mi	miles	1.61	kilometers	km	kilometers	0.621	miles	mi
AREA								
in ²	square inches	645.2	square millimeters	mm ²	square millimeters	0.0016	square inches	in ²
ft ²	square feet	0.093	square meters	m ²	square meters	10.764	square feet	ft ²
yd ²	square yards	0.836	square meters	m ²	square meters	1.195	square yards	yd ²
ac	acres	0.405	hectares	ha	hectares	2.47	acres	ac
mi ²	square miles	2.59	square kilometers	km ²	square kilometers	0.386	square miles	mi ²
VOLUME								
fl oz	fluid ounces	29.57	milliliters	mL	milliliters	0.034	fluid ounces	fl oz
gal	gallons	3.785	liters	L	liters	0.264	gallons	gal
ft ³	cubic feet	0.028	cubic meters	m ³	cubic meters	35.71	cubic feet	ft ³
yd ³	cubic yards	0.765	cubic meters	m ³	cubic meters	1.307	cubic yards	yd ³
NOTE: Volumes greater than 1000 l shall be shown in m ³ .								
MASS								
oz	ounces	28.35	grams	g	grams	0.035	ounces	oz
lb	pounds	0.454	kilograms	kg	kilograms	2.202	pounds	lb
T	short tons (2000 lb)	0.907	megagrams (or "metric ton")	Mg (or "t")	megagrams (or "metric ton")	1.103	short tons (2000 lb)	T
TEMPERATURE (exact)								
°F	Fahrenheit temperature	5(F-32)/9 or (F-32)/1.8	Celcius temperature	°C	Celcius temperature	1.8C + 32	Fahrenheit temperature	°F
ILLUMINATION								
fc	foot-candles	10.76	lux	lx	lux	0.0929	foot-candles	fc
f	foot-Lamberts	3.426	candela/m ²	cd/m ²	candela/m ²	0.2919	foot-Lamberts	f
FORCE and PRESSURE or STRESS								
lbf	poundforce	4.45	newtons	N	newtons	0.225	poundforce	lbf
lbf/in ²	poundforce per square inch	6.89	kilopascals	kPa	kilopascals	0.145	poundforce per square inch	lbf/in ²

* SI is the symbol for the International System of Units. Appropriate rounding should be made to comply with Section 4 of ASTM E380. (Revised September 1993)

EFFECTS OF GRADATION AND COHESION ON BRIDGE SCOUR

VOLUME II

TABLE OF CONTENTS

I. INTRODUCTION AND OBJECTIVES	1
1.1 Introduction	1
1.2 Objectives	2
II. SCOUR AROUND BRIDGE PIERS	4
2.1 Definition and classification of scour	4
2.2 Clear water and live bed scour	5
2.3 Flow pattern at a cylindrical pier	8
2.4 Analysis of the clear water scour parameters	10
III. REVIEW OF LITERATURE ON LOCAL SCOUR	11
IV. EXPERIMENTAL SETUP AND PROCEDURE	31
4.1 The flume	31
4.2 Individual measurements	34
4.2.1 Discharge	34
4.2.2 Flow depth	34
4.2.3 Slope	35
4.3 Sediment mixture	35
4.4 Description of testing procedure	39
V. RESULTS AND DISCUSSION OF RESULTS	42
5.1 Scour in steady (long duration) flow	42

5.1.1	Contraction scour	42
5.1.2	Local pier scour	42
5.1.2.1	Maximum local scour for uniform material	43
5.1.2.2	Maximum local scour for highly graded material ($\sigma_g = 3.7$)	49
5.1.2.3	Maximum local scour for moderately graded material ($\sigma_g = 2.17$)	52
5.1.3	The coefficient of gradation	55
5.2	Scour in unsteady flow (discretized hydrograph)	59
VI.	SUMMARY AND CONCLUSIONS	68
6.1	Conclusive consideration	68
6.2	Suggestions for further research	71
	BIBLIOGRAPHY	72
	APPENDIX A Hydraulic data measurements	75

EFFECTS OF GRADATION AND COHESION ON BRIDGE SCOUR

VOLUME II

LIST OF FIGURES

Figure 2.1	Shields chart for threshold condition of uniform sediments	6
Figure 2.2	Flow chart to calculate limiting armor velocity, (U_a)	7
Figure 2.3	The flow patterns at a cylindrical pier	9
Figure 3.1	Coefficient of gradation	21
Figure 3.2	Coefficient of sediment size	21
Figure 3.3	Correlation between (Y_s / b) and (D_{50} / b), ($U_* t / b$), ($v / U_* b$)	22
Figure 3.4	Influence of flow intensity on scour depth	24
Figure 3.5	Influence of flow depth on scour depth	25
Figure 3.6	Influence of sediment size on scour depth	26
Figure 3.7	Alignment factor for piers	27
Figure 3.8	Flow chart for determination of design scour depth	28
Figure 3.9	Correlation between (Y_s / b) and (Y_1 / b) for cylindrical piers	29
Figure 4.1	Schematic diagram for the 2.0 ft flume	33
Figure 4.2	Gradation curves for sediment mixtures	38
Figure 4.3	The 5.0 minute discretized hydrograph for the two different peaks	40
Figure 5.1	Measured and fitted (Y_s / Y_1) for uniform bed material	48
Figure 5.2	Measured and fitted (Y_s / Y_1) for highly graded mixture	51
Figure 5.3	Measured and fitted (Y_s / Y_1) for moderately graded mixture	54
Figure 5.4	Comparison between K_g of Raudkivi (1986) and Eq. 5.6	57

Figure 5.5	Coefficient of gradation values from Eq. 5.6	58
Figure 5.6	Measured and fitted values for the 5.0 min. hydrograph	61
Figure 5.7	Relationship between the 2.5, 5.0, and 7.5 min. hydrographs	65
Figure 5.8	Measured Y_r/Y_1 for the 2.5 min, hydrograph and the flash flood	67

EFFECTS OF GRADATION AND COHESION ON BRIDGE SCOUR

VOLUME II

LIST OF TABLES

Table 2.1	Exponent m	7
Table 3.1	Pier shape factors	27
Table 4.1	Grain size distribution for sediment mixture	37
Table 5.1	Output of the regression equations for uniform mixtures	45
Table 5.1(a)	Output of the regression equations for uniform mixture $D_{50}= 1.87$ mm ..	46
Table 5.1(b)	Output of the regression equations for uniform mixture $D_{50}= 0.76$ mm ..	47
Table 5.2	Output of the regression equations for mixture (1)	50
Table 5.3	Output of the regression equations for mixture (3)	53
Table 5.4	Output of the regression equations for the determination of K_g	56
Table 5.5	Output of the regression equations for the determination of the relationship between the steady and the 5 min. peak flow	60
Table 5.6	Output of the regression equations for the relationship between the 2.5 and 5 min. peak flows	63
Table 5.7	Output of the regression equations for the relationship between the 7.5 and 5 min. peak flows	64

LIST OF SYMBOLS

b	Pier width
d	Sediment diameter
D_{max}	Sediment diameter
D_{15}	Sediment size at which 15% of material is finer
D_{50}	Sediment size at which 50% of material is finer
D_{85}	Sediment size at which 85% of material is finer
D_{90}	Sediment size at which 90% of material is finer
f	Lacey's silt factor
Fr	Froude number
Fr_a	Approach Froude number, $U / (gY_1)^{1/2}$
Fr_c	Critical Froude number, $U_c / (gY_c)^{1/2}$
g	Gravitational acceleration
H_s	Depth of scour measured from water surface
K	Coefficient of sediment size
K_g	Coefficient depending on the bed material gradation
K_I	Flow intensity coefficient
K_s	Pier shape coefficient
K_y	Flow depth ratio
K_a	Pier alignment coefficient
L	Length of pier
N_s	Sediment number, it is a measure of the strength of the vortex-bed interaction

q	Discharge per unit width
Q	Flow discharge
r	Ratio of the depth of scour at the pier to the depth of scour at long contraction
R_c	Reynolds number
S_s	Sediment specific gravity
t	Time
U	Mean velocity of the undisturbed flow
U_a	Limiting armor velocity
U_{ca}	Armoring critical velocity
U_c	Critical velocity
U_*	Shear velocity
U_{*c}	Critical shear velocity
x	Correction factor accounting for effect of viscosity
Y_1	Approach flow depth
Y_s	Scour depth
Y_{sc}	Equilibrium scour depth
α	Flow angle of attack
Δt	Discretization time step
ν	Kinematic viscosity
ρ	Water density
ρ_s	Sediment density
τ_c	Critical shear stress
τ_o'	Maximum shear stress in a contraction

CHAPTER I.

INTRODUCTION AND OBJECTIVES.

1.1 Introduction.

If the foundations of a bridge are meant to be supported by the alluvial material of a river bed, the knowledge or at least the estimation as accurate as possible of maximum possible scour depth is a real important step in the design of bridge foundations. Predicting the maximum scour depth for the bridge foundations, the foundations can be designed such that the probability of scour seriously disturbing the stability of the bridge is balanced against the cost of replacing the whole bridge and the risk of unsafety. Accurately predicting the value of the maximum scour depth will confine the risk of failure to the probability of exceeding the design flood.

In a general sense, scour is the erosive action of running water in streams that carries away bed and bank material. Scour at bridges can be classified as local scour at piers and abutments, contraction scour, and aggradation and degradation of the river bed. Furthermore, the type of local scour can be classified as live bed scour and clear water scour.

In order to design fail safe foundations, a number of equations for predicting scour depth around bridge foundations were proposed by different researchers over the last fifty years. In this study clear water local scour around bridge piers is the main interest. Local scour was observed to be a function of flow variables, pier geometry and

alignment, time and bed material characteristics. Most investigators have attempted to develop relationships for the maximum scour depth in steady flow, and these are used for design. However, the flow in a river during a flood is unsteady, and discharge changes are quite rapid. In natural streams at peak discharges the unsteadiness of flow is pronounced, and the maximum scour depth for a given discharge will not be reached when the discharge does not run for a long time. Therefore, it is more convenient to study the scour caused by a hydrograph while checking the safety of bridge foundations along its remaining service life.

Furthermore, the bed material of streams are almost always nonuniform. In a rational approach for determination of scour depth, factors of nonuniformity of bed material must be taken into consideration.

Only Harwood (1977), Walker (1978), Verstappen (1978), Yanmaz and Altinbilek (1991), and Kothyari (1992) have studied scour during unsteady flows to a limited extent. Similarly, Raudkivi and Ettema (1983) have made some attempts to study the effect of sediment gradation on scour depth.

The main interest of this study is to investigate the variation of local scour depth around circular bridge piers during steady and unsteady clear water flows in uniform and nonuniform sediments.

1.2 Objectives.

A flume study was conducted to achieve four main objectives. The first objective is to develop a prediction model for the clear water scour depth around circular bridge

piers for uniform bed material. The second objective of this study is to investigate the effect of bed material gradation on the clear water scour depth. The third objective is to examine the relation between the maximum scour depth of a steady long-duration flow and the corresponding scour depth of a simulated (discretized) hydrograph having the same peak discharge as the steady discharge. The fourth objective is to examine the relation between different discretized hydrographs, i.e same peak discharge but different time step discretization.

In order to meet this objectives a physical model study was conducted and thirty four runs using four different bed material mixtures were made at the Engineering Research Center Hydraulics Laboratory of Colorado State University. In each of these runs scour and flow conditions data were measured around the three circular piers placed along the flume.

CHAPTER II.

SCOUR AROUND BRIDGE PIERS.

2.1 Definition and classification of scour.

Scour is a natural phenomenon caused by the erosive action of flowing water on the bed and banks of alluvial streams. The type of scour that may occur at a bridge site could be classified into the following three classes:

1. Aggradation and degradation, which is the long term general scour of the stream that would occur whether the bridge exists or not.
2. Contraction scour (localized scour) resulting from the constriction of the waterway by the bridge.
3. Local scour, which is caused by the interference with flow by the bridge piers and abutments.

The general basic characteristics of local scour is well stated by Laursen (1952):

- "1. The rate of scour will equal the difference between the capacity for transport out of the scoured area and the rate of supply of the material.
2. The rate of scour will decrease as the flow section is enlarged.
3. There will be a limiting extent to scour.
4. This limit will be approached asymptotically."

Furthermore, local scour can be classified into two classes according to the movement of the bed material upstream of piers or abutments. The two classes are clear water and live bed scour.

2.2 Clear water and live bed scour.

The threshold conditions for uniform sediments is effectively determined by Shields diagram (Henderson 1966). For given fluid density and viscosity and sediment density, the Shields diagram can be used to obtain a plot of the critical shear velocity U_{*c} against grain size D_{50} as shown in Fig. 2.1. Water and sediment densities of 1.0 t/m^3 and 2.65 t/m^3 respectively, have been assumed in the development of Fig. 2.1. Threshold shear velocity is converted to threshold mean flow velocity U_c using, as an approximation, the logarithmic form of the velocity profile

$$\frac{U_c}{U_{*c}} = 5.75 \log\left(5.53 \frac{Y_1}{D_{50}}\right) \quad (1.1)$$

where Y_1 is the flow depth. For uniform sediments, U_c will mark the transition from the clear water to live bed scour conditions.

For nonuniform sediments U_c will depend upon both the median grain size D_{50} and the geometric standard deviation σ_g . With nonuniform sediments, a flow can disturb the grains, removing some but simply rearranging others into an armored bed and stabilizes. For such case the flow is still considered in a clear water stage.

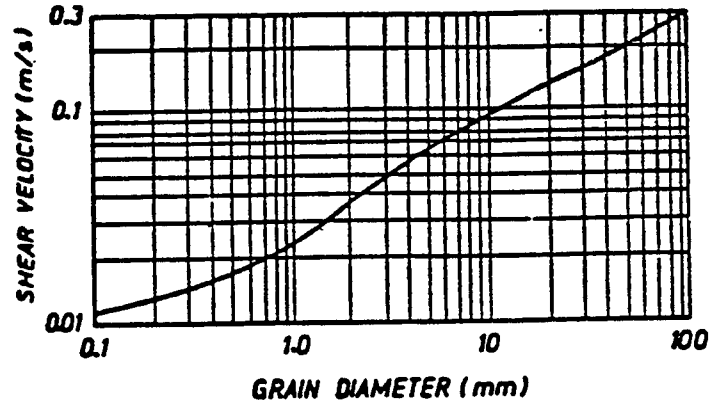


Fig. 2.1 Shields chart for threshold condition of uniform sediments

The flow condition beyond which armoring of a nonuniform channel bed is impossible is termed the limiting armor condition. This condition represents the coarsest or most stable armored bed for the given bed material. At flows greater than U_{ca} , no armor layer can form and the flow is then considered to be in a live-bed stage. For a given D_{50} , U_{ca} increases with increasing σ_g . Chin (1985) showed that the value of U_{ca} for a given sediment is dependent on the maximum D_{max} size and gives a method to determine U_{ca} using D_{max} , which can be found from D_{50} and σ_g if a logarithmic normal distribution is assumed:

$$D_{max} = \sigma_g^m D_{50} \quad (2.2)$$

Where m depends upon the size chosen for D_{max} as shown in table 2.1. The method of evaluation of U_a which is the appropriate flow velocity to characterize the limiting armor

condition for scour determination, Baker (1986), is summarized in the flow chart of Fig.

2.2.

Table 2.1 Exponent m

Assumed value of D_{max} (1)	m (2)
D_{90}	1.28
D_{75}	1.65
D_{50}	2.06
D_{30}	2.34

INPUT DATA:

GRAIN SIZE DISTRIBUTION, D_{50} , σ_g , D_{max}
FLOW DEPTH, y

CALCULATE $D_{50a} = D_{max} / 1.8$

FIND U_{nc} , U_{ca} from Fig.2.1
using D_{50} , D_{50a}

FIND U_c , U_{ca} using
 U_{nc} , U_{ca} in eq.2.1

CALCULATE $U_a = 0.8U_{ca}$

CHECK $U_a \geq U_c$

Fig. 2.2 Flow chart to calculate limiting armor velocity, (U_a)

For nonuniform sediments, U_a is considered to mark the transition from clear-water to live-bed scour conditions.

2.3 Flow pattern at a cylindrical pier.

The dominant feature of the flow around a pier is the development of systems of vortices. Depending on the pier's shape and geometry, and free stream conditions at the upstream, the systems of vortices can be composed of any, all, or none of three basic systems: the horseshoe vortex system, the wake vortex system, and the trailing vortex system.

Along the upstream element of the cylinder, which is the stagnation line, the velocity is zero and the stagnation pressure is $\rho U^2/2$. Hence, the decreasing velocity, from the free surface down to zero at the bed, causes the stagnation pressure to sharply decrease. This downward pressure gradient drives the down flow. If the field of the pressure gradient is sufficiently strong, it causes a three dimensional separation of the boundary layer. Then the horseshoe vortex develops as result of the separation and extends downstream past the sides of the pier for a distance of few pier widths.

Moving from the stagnation line around the cylinder, the tangential component of velocity increases to a maximum of about twice the free stream velocity at the maximum breadth point. In this vicinity the flow separates from the cylinder, producing the wake zone of relatively low velocities. The normal pressure along the surface of the cylinder decreases from its maximum at the stagnation line to zero, or the static pressure. The normal pressure then continues to decrease and becomes negative, that is, less than the free stream pressure by an increasing magnitude, until the separation point is reached. The wake vortex system is formed by the rolling up of the unstable shear layers generated at the surface of the pier. The shear layers are detached from either side of the pier at

the separation line. The wake vortex system causes large scour holes to develop in the case of the horseshoe vortex system is adequately controlled. The wake vortex system acts somewhat like a vacuum cleaner in removing the bed material. The bed material is carried downstream by the eddies shedding from the pier.

The trailing vortex system usually occurs only on complete submerged piers and is composed of one or more discrete vortices attached to the top of the pier and extending downstream. These vortices form when finite pressure differences exist between two surfaces meeting at a corner, such as the top of the pier.

Finally, a bow wave develops at the surface with rotation in the opposite sense to that in the horseshoe vortex. The bow wave can become important in relatively shallow flows where it interferes with the approach flow and causes a reduction in the strength of the down flow. Fig. 2.3 shows the flow patterns at a cylindrical pier.

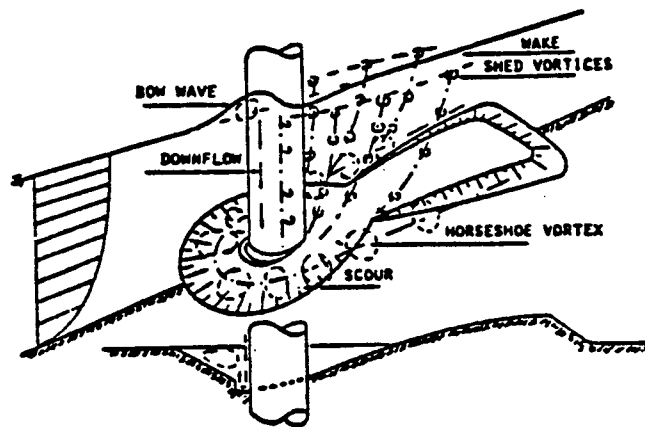


Fig. 2.3 The flow patterns at a cylindrical pier

2.4 Analysis of the clear water scour parameters.

The many parameters which control the scour process around bridge piers can be arranged into four groups:

1. fluid parameters: fluid density, and fluid viscosity.
2. flow parameters: mean approaching velocity, approaching flow depth, and bed roughness.
3. bed material parameters: particle size and shape, bed material gradation, and density of particles.
4. pier parameter: pier dimensions, pier shape, piers spacing, and pier surface roughness.

Because of the complexities of analyzing all of the above parameters, many investigators stated the validity of the following assumptions: the difference between the laboratory and field values for density and viscosity can be neglected; streams can be considered sufficiently wide so that the pier spacing and respectively the contraction can be neglected; the piers are perfectly smooth.

These assumptions reduce the parameters affecting the clear water scour around a circular pier to the following :

1. fluid density ρ and fluid viscosity μ .
2. Mean velocity of approach flow U and approaching flow depth Y .
3. particle mean diameter D_{50} , bed material gradation presented as the geometric standard deviation of the particle size distribution σ_g , and particle density ρ_s .
4. pier width b .

CHAPTER III.

REVIEW OF LITERATURE ON LOCAL SCOUR.

A number of equations for predicting local scour depth were proposed by different researchers over the last fifty years. The equations are based on three methods of analysis. These methods are:

1. The regime approach, by using the transport relations in the approaching flow and in the scour hole.
2. Regression analysis of the available data, to present empirical equations.
3. Dimensional analysis of the basic parameters affecting the local scour process.

Some of the formulae developed to predict the anticipated depth of local scour at intermediate bridge piers follow.

The Inglis-Poona equation (1938)

$$\frac{H_s}{b} = 1.70 \left(\frac{q}{b}\right)^{0.78} \quad (3.1)$$

in which

H_s = depth of scour from water surface;

b = pier width.

(ft-units), the equation was based on series of model studies of the rectangular round-nosed pier of the Hardinge bridge (India) without general movement of the bed. This relation is not dimensionally correct and cannot therefore be utilized for general applications. The equation considered only the Ganga sand of mean diameter of 0.29 mm.

Chitale's formula (1944)

$$\frac{Y_s}{Y_1} = 6.65 Fr - 5.49 Fr^2 - 0.51 \quad (3.2)$$

in which

Fr = approach flow Froude number; $Fr = U/(gY_1)^{1/2}$

U = mean velocity of approach flow;

Y_s = maximum scour depth; and

Y_1 = flow depth.

The equation was based on the results of an extension of the original Poona model tests of the Hardinge bridge (India). The equation was derived for clear water scour, $0.1 \leq Fr \leq 0.45$, and sand diameter of 0.16 to 1.51 mm. The equation did not take into consideration the effect of bed material gradation.

The Inglis Lacey relationship (1949)

$$H_s = 0.946 \left(\frac{Q}{f}\right)^{\frac{1}{3}} \quad (3.3)$$

in which

Q = discharge, in cfs;

f = Lacey's silt factor = $1.76 (D_{50})^{1/2}$; and

D_{50} = mean diameter of bed material, in mm.

The equation is dimensionally inhomogeneous. It simply states that the scour depth measured from the water surface is twice the Lacey regime depth. The principal restriction of this relationship is that of the regime channel. The equation does not consider the effect of bed material gradation.

Laursen and Toch's formula (1956)

$$\frac{Y_s}{b} = 1.35 \left(\frac{Y_1}{b}\right)^{0.30} \quad (3.4)$$

The formula was based on experiments that was conducted to investigate the influence of pier shape, angle of attack, water depth, velocity and sediment size. Laursen and Toch concluded that there was no systematic influence of sediment size and velocity in the range studied. The formula is valid for live bed scour.

Laursen's relationship (1962)

$$\frac{b}{Y_1} = 5.5 \frac{Y_s}{Y_1} \left[\left(\frac{Y_s}{rY_1} + 1 \right)^{1.7} - 1 \right] \quad (3.5)$$

in which

r = the ratio of the depth of scour at the pier to the depth of scour which would occur in a long contraction.

The equation was based on an analysis adapting the solution of the long contraction scour, with balance of sediment transport capacity in the normal and contracted sections, to the pier. A second relationship

$$\frac{b}{Y_1} = 5.5 \frac{Y_s}{Y_1} \left[\frac{\left(\frac{Y_s}{rY_1} + 1 \right)^{\frac{7}{6}}}{\left(\frac{\tau_o'}{\tau_c} \right)^{\frac{1}{2}}} - 1 \right] \quad (3.6)$$

in which

τ_o' = the maximum shear stress in the contraction;

τ_c = the critical shear stress in the contraction; where

$$\tau_o'/\tau_c = U_1^2/120(D_{50})^{2/3} Y_1^{1/3}.$$

This relationship was similarly adapted from clear water scour analysis of the long contraction in which the contraction scoured to give a boundary shear equal to the critical

shear for the bed material, and the shear in the approach was less than this value.

Larras's formula (1963)

$$Y_{sc} = 1.05 k b^{0.75} \quad (3.7)$$

in which

Y_{sc} = the equilibrium scour depth;

k = coefficient depend on pier shape; suggested to be 1.0 for circular piers and 1.4 for rectangular piers aligned with the flow direction.

(m-units), the formula was based on scour data by Chabert and Engeldinger (1956). The effect of pier alignment was considered and given in tables. The formula represent the maximum scour depth near the threshold velocity of the undisturbed bed material as a function of pier diameter. The formula neglected the effect of water depth, grain size, and the grain size distribution.

Neill's equation (1964)

$$\frac{Y_s}{b} = 1.5 \left(\frac{Y_1}{b}\right)^{0.3} \quad (3.8)$$

The equation was based on live bed scour data by Laursen and Toch (1956) describing the influence of water depth, mean flow velocity and sediment size, on a rectangular pier of 0.06 m width at angle of attack of 30°. The data showed the non systematic influence of grain size and velocity in the range studied. For round-nosed piers the coefficient should be changed to 1.2 instead of 1.5.

Breusers (1965) proposed

$$Y_{sc} = 1.4 b \quad (3.9)$$

for scour around circular piers in case of live bed scour. The equation neglected all the parameters affecting the scour except for the pier width.

Arunachalam (1965)

$$\frac{Y_1 + Y_s}{Y_r} = 1.95 \left(\frac{b}{Y_r}\right)^{\frac{1}{6}} \quad (3.10)$$

in which

Y_r = the regime depth; $Y_r = 0.9 q^{2/3}$ (ft-units) or $Y_r = 1.334 q^{2/3}$ (m-units).

The equation is based on the Inglis (1948) data with the aid of Kennedy-relationship that states: $U = 0.84 Y_r^{0.34}$ (ft-units). A contradiction applies because the conditions of the Poona tests were those of clear water scour and regime theory implies up to moderate rate of sediment movement.

Hancu's equation (1965)

$$\frac{Y_{sc}}{b} = 3.3 \left(\frac{D_{50}}{b}\right)^{0.2} \left(\frac{Y_1}{b}\right)^{0.13} \quad (3.11)$$

The equation is based on experimental results of circular piers of diameters ranging from 3 to 20 cm in coarse material ($D_{50} = 0.5, 2$ and 5 mm). The equations considered the

grain size but on the other hand it does not take into account the effect of grain size distribution.

Shen's equations (1966, 1969)

$$Y_s = 0.000059 R_e^{0.512} \quad (3.12)$$

$$Y_s = 0.00022 R_e^{0.619} \quad (3.13)$$

in which

R_e = Reynolds number based on the pier diameter; $R_e = Ub/\nu$.

(m-units), the equations are based on experimental data of circular piers of diameters 0.15 and 0.9 m, and particle mean diameters of 0.24 and 0.46 mm. Shen also used other results from literature to derive these to relationships. This relation must be considered as an upper envelope to scour depth expected.

Coleman formula (1971)

$$\frac{Y_s}{b} = 1.49 \left(\frac{U^2}{gY_1} \right)^{\frac{1}{10}} \quad (3.14)$$

The formula was based on data from Shen et al (1969) and results from experiments on circular piers with diameters of 0.045 and 0.076 m in sand with mean diameter of 0.10 mm. The formula predict the scour depth in case of live bed scour. It is clear that the equation did not take into account the effect of grain size or gradation.

Nicollet (1971)

Nicollet extended the experiments by Chabert and Engeldinger (1956) to consider more variables. He tried to explain more the effect of grain size and gradation. He performed tests with grain sizes of 0.94, 1.93, 3, 7, 15 and 25 mm. He concluded that the maximum scour depth increases with grain size up to mean diameter of 2.0 mm for constant approaching water depth. He also did some tests with widely graded material ($D_5=0.24$ mm, $D_{50}=0.7$ mm, $D_{90}=4.0$ mm), and concluded that the maximum scour depth is much lower for the graded material than for the uniform material under similar conditions.

CSU's equation (1975)

$$\frac{Y_s}{Y_1} = 2.0 K_1 K_2 \left(\frac{b}{Y_1}\right)^{0.65} (Fr)^{0.43} \quad (3.15)$$

in which

K_1 = correction for pier shape (equal to 1.0 for circular piers), from tables; ranging from 0.9 for sharp nose to 1.1 for square nose, and

K_2 = correction for angle of attack of flow (equal to 1.0 for circular piers), from tables.

The equation is based on both dimensional analysis of the parameters affecting pier scour and the analysis of laboratory data. The equation is valid for both live bed and clear water scour. The equation did not take into account the effect of bed material size and gradation.

Basak et al (1975)

$$Y_{sc} = 0.558 b^{0.586} \quad (3.16)$$

Based on experiments with square piers with width ranging from 0.04 to 0.5 m in coarse sand with mean diameter of 0.65 mm. The water depths were small (up to 0.14 m) and for most of the tests $U > U_c$. As both depth and velocity were varied simultaneously, no independent variation of parameters was obtained. Basak concluded that the maximum scour depth is only pier width dependent. The equation ignored the effect of grain size and gradation.

Jain's formula (1981)

$$\frac{Y_s}{b} = 1.84 \left(\frac{Y_1}{b}\right)^{0.30} (Fr_c)^{0.25} \quad (3.17)$$

in which

Fr_c = the critical Froude number for the bed material based on the threshold velocity from Sheild's criterion for critical shear stress and the logarithmic velocity distribution, $U_c/U_{*c} = 2.5 \ln(11.02 Y_1 x/D_{50})$;

U_c = the critical velocity for the beginning of bed particle motion, (threshold velocity);

U_{*c} = the critical shear velocity;

x = correction factor accounting for the effect of viscosity.

The formula is valid for clear water scour around cylindrical piers. The formula is based on comparison of several predictors for the maximum clear water scour depth and the available experimental data. The comparison indicated that the scour formula by Laursen and Toch (1956) is the best predictor among those compared. The formula represents an envelop for the maximum clear water scour depth which is very similar to that of Laursen and Toch (1956) but it includes the effect of sediment size on scour depth.

Baker's formula (1981)

$$\frac{Y_s}{b} = [g_1 \frac{U}{U_c}] [K_1 \tanh(K_2 \frac{Y_1}{b})] [g_2 g_3] \quad (3.18)$$

in which

K_1 and K_2 = functions of $(\rho_s - \rho)gD_{50}^3/(\rho v^2)$;

g_1 = function of U/U_c ; and

g_2 and g_3 = function of shape and alignment of the pier.

The formula was based on a study of the mechanism of the vortex in the scour hole for $U/U_c < 1$, and the use of experimental results.

Raudkivi and Ettema (1977, 1983, 1986)

$$\frac{Y_{sc}}{Y_1} = 2.3 K_s \quad (3.19)$$

in which

K_g = correction factor for the effect of sediment gradation depends on σ_g ; and

σ_g = the geometric standard deviation of the bed material size distribution.

Raudkivi and Ettema proposed values for the correction factor of sediment gradation, K_g , and sediment size, K , as shown in Fig. 3.1 and 3.2.

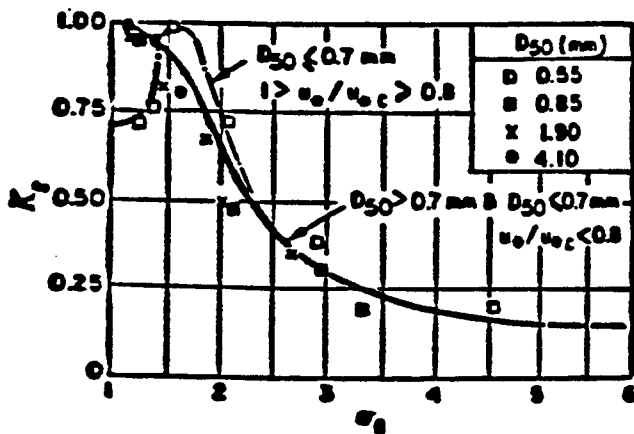


Fig. 3.1 Coefficient of gradation

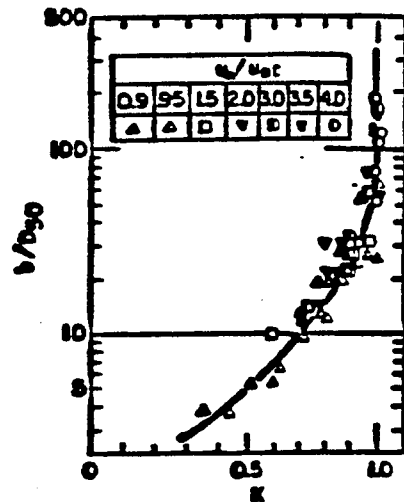


Fig. 3.2 Coefficient of sediment size

Although many studies of local scour were reported in the literature, the number of studies dealing with the time variation of scour depth around bridge piers was very limited. Raudkivi and Ettema presented sets of curves as a function of σ_g that relate the relative clear water scour depth to the nondimensional time term ($u_c t/b$), Strouhal number, together with the sediment based Reynolds number, and the relative sediment

Fig. 3.3 appear to define three straight-line segments on the semi-logarithmic plot. The first segment is associated with the rapid scouring by the down flow. The down flow excavates a groove around the perimeter of the pier. The middle segment describes the development of the scour hole as the horseshoe vortex moves away from the cylinder and grows in strength. The last segment indicates the equilibrium depth. As σ_g increases, the middle segments gradually vanish leaving only two segments.

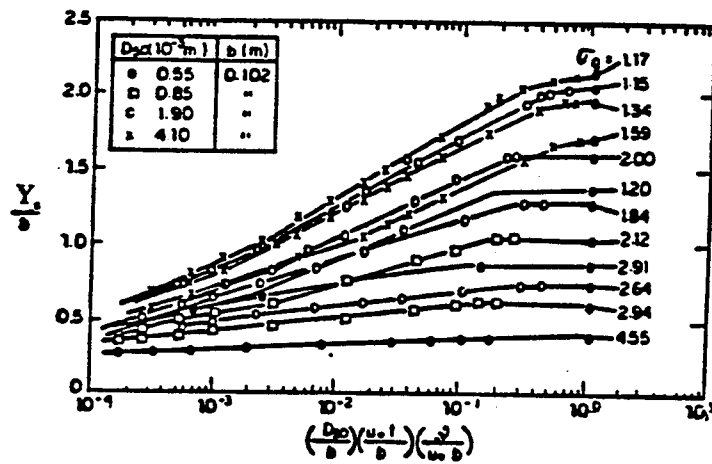


Fig. 3.3 Correlation between Y_s/b and $(D_{50}/b) (U_* t/b) (v/U_* b)$

Eroehlich's formula (1987)

$$\frac{Y_s}{b} = 0.32 K_1 \left(\frac{b'}{b}\right)^{0.62} \left(\frac{Y_1}{b}\right)^{0.46} (Fr)^{0.2} \left(\frac{b}{D_{50}}\right)^{0.08} + 1.0 \quad (3.20)$$

in which

K_1 = coefficient for pier type, $K_1 = 1.0$ for cylindrical pier;

b' = pier width projected normal to the approach flow, $b' = a \cos\alpha + L \sin\alpha$;

α = angle of attack; and

L = pier length.

The formula was based on linear regression analysis of pier live bed scour. The addition of one to the equation is to give a factor of safety for design purposes. The formula did not account for the effect of sediment gradation.

B. W. Melville and A. J. Sutherland's formula (1988)

$$\frac{Y_s}{b} = K_1 K_y K_d K_g K_s K_\alpha \quad (3.21)$$

in which

K_1 = flow intensity coefficient;

K_y = flow depth ratio;

K_d = sediment size;

K_g = sediment gradation;

K_s = pier shape coefficient; and

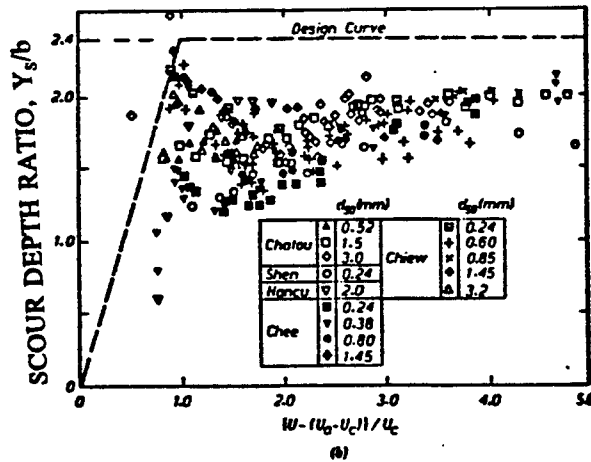
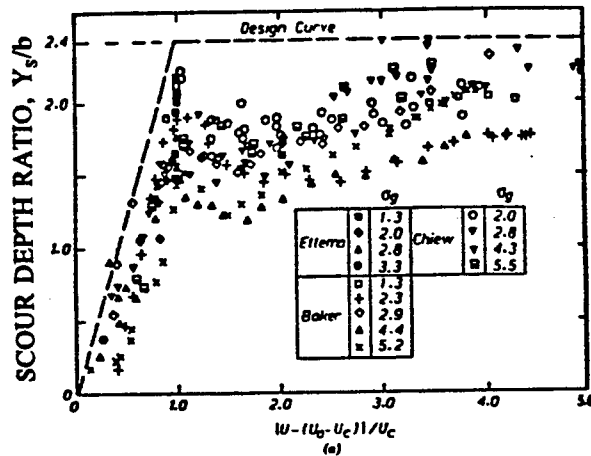
K_α = pier alignment coefficient.

The formula was based on dimensional analysis of parameters affecting the local scour.

Each factor was then considered individually as follows.

Flow Intensity

The flow intensity factor determines the scouring processes that are important. The appropriate form for this factor is $(U - (U_s - U_c)) / U_c$ for nonuniform sediment, and U / U_c for uniform sediment. For values larger than one live-bed scour occurs, while the clear-water scour pertains for values smaller than one. Fig. 3.4 shows the influence of flow intensity on scour depth.



a) graded material b) uniform material

Fig. 3.4 Influence of flow intensity on scour depth

Flow Depth Ratio

Scour depth increases with flow depth up to limiting value of the flow depth ratio Y_1/b , beyond which there is no influence of flow depth. The flow depth factor K_y , shown in Fig. 3.5, is the ratio of Y_s/b at a particular value of Y_1/b to that at $Y_1/b \geq 4$. These data all have $b/D_{50} \geq 50$.

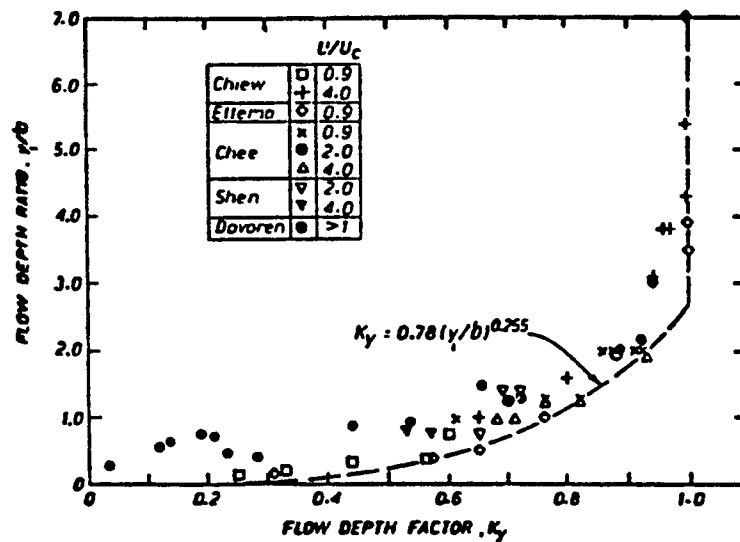


Fig. 3.5 Influence of flow depth on scour depth

Sediment Size Ratio

Chiew's (1984) live-bed data for uniform sediments and those of Ettema (1980) derived from clear-water flows delineate the effects of the sediment size ratio b/D_{50} on scour depth as shown in Fig. 3.6. K_d , the sediment size factor, is the ratio of Y_s/b at a particular value of b/D_{50} to that at $b/D_{50} \geq 50$, beyond which there is no effect of sediment size.

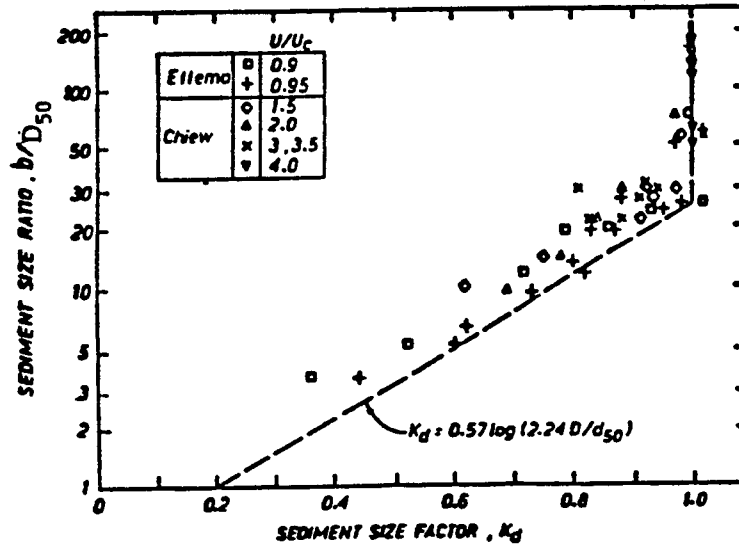


Fig. 3.6 Influence of sediment size on scour depth

Sediment Gradation Effects

Work by Ettema (1976) showed that the scour depths are reduced dramatically as σ_g increases, for the case of clear-water scour depths. The effects of σ_g have been largely accounted for by the introduction of U_a into the abscissa.

Shape and Alignment Effects

Factors to account for shape are given in Table 3.1. These were based on aligned piers with the flow, and $K_s = 1.0$ for cylindrical piers.

Table 3.1 Pier shape factors

Shape in plan (1)	Length/ width (2)	Reference			
		Tison (1940) (3)	Laursen and Tech (1958) (4)	Chabert and Engeldinger (1956) (5)	Venkatesh (1968) (6)
Circular	1.0	1.0	1.0	1.0	1.0
Lenticular	2.0	—	0.97	—	—
	3.0	—	0.76	—	—
	4.0	0.67	—	0.73	—
	7.0	0.41	—	—	—
Parabolic nose	—	—	—	—	0.56
Triangular nose, 60°	—	—	—	—	0.75
Triangular nose, 90°	—	—	—	—	1.25
Elliptic	2.0	—	0.91	—	—
	3.0	—	0.83	—	—
Ogival	4.0	0.86	—	0.92	—
Joukowski	4.0	—	—	0.86	—
	4.1	0.76	—	—	—
Rectangular	2.0	—	1.11	—	—
	4.0	1.40	—	1.11	—
	6.0	—	1.11	—	—

Alignment factors K_a taken from Laursen (1958) are shown in Fig. 3.7.

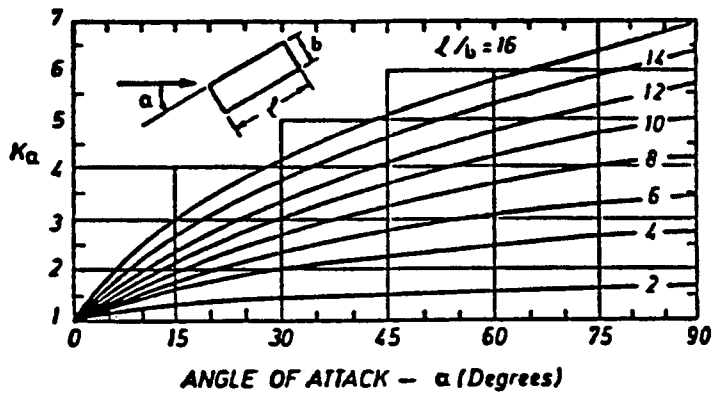


Fig. 3.7 Alignment factor for piers

The method was summarized in flow chart form in Fig. 3.8.

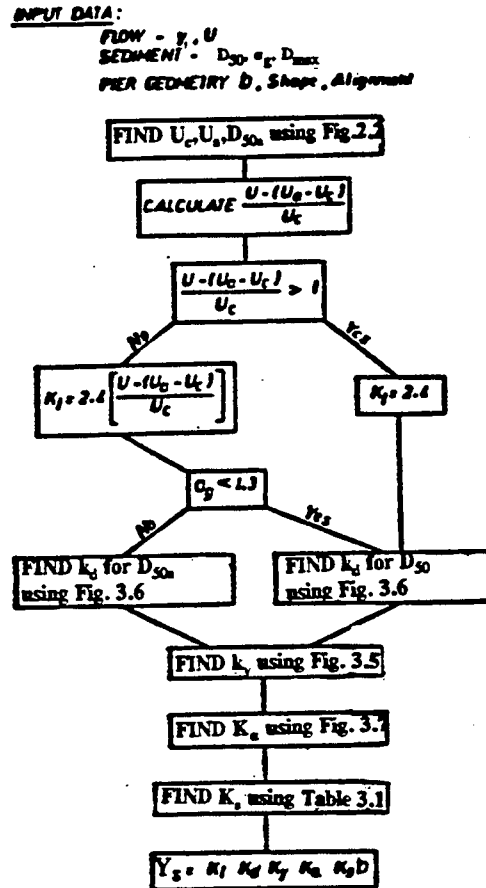


Fig. 3.8 Flow chart for determination of design scour depth

GÜNYAKTI (1989)

Under the conditions of cohesionless uniform bed material, single pier, long flow duration, wide channel, and flow velocities close to the threshold conditions Yanmaz (1989), Breusers et al. (1977), Chiew and Melville (1987), Mellville and Sutherland (1988), Günyakti (1989), and Yanmaz (1989) presented curves relating Y_s/b to Y_1/b . Günyakti (1989) developed the curve enveloping the data points in Fig. 3.9. The curve represent the upper boundary of the available scour depth data reported in the literature.

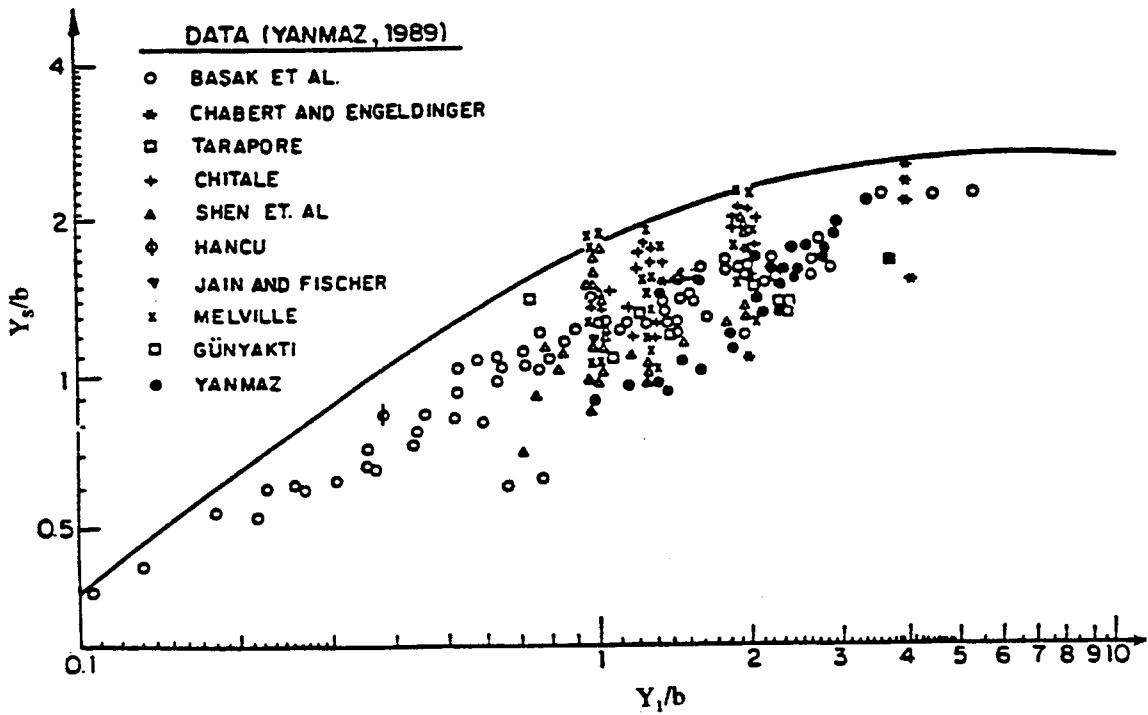


Fig. 3.9 Correlation between Y_s/b and Y_1/b for cylindrical piers

The effects of sediment size and gradation can be taken into account to modify the results obtained from Fig. 3.9 that represents uniform materials. Gunyakti suggested the use of Raudkivi and Ettema's correction factors (1983) for the effects of sediment size and sediment gradation.

Kothyari et al. equation (1992)

$$\frac{Y_s}{b} = 0.66 \left(\frac{b}{d}\right)^{-0.25} \left(\frac{Y_1}{d}\right)^{0.16} \left(\frac{U^2 - U_c^2}{\frac{\Delta \gamma_s d}{\rho}}\right)^{0.4} \alpha^{-0.3} \quad (3.22)$$

in which

d = sediment diameter; where $d = D_{50}$ if $\sigma_g < 1.124$ and $d = 0.925 \sigma_g D_{50}$;

$\Delta \gamma_s$ = difference between the sediment specific weight and water specific weight;

and

α = opening ratio.

The equation is based on the analysis of the primary vortex developing in the front of the pier. A mathematical model was developed to estimate the temporal variation of scour depth in uniform, nonuniform and stratified sediments. This equation for the estimation of maximum scour depth was obtained from the model as the scour depth at large time. The equation is applicable only when $U > U_c$.

CHAPTER IV

EXPERIMENTAL SETUP AND PROCEDURE

A series of flume experiments was conducted at the Engineering Research Center of Colorado State University in the Hydraulics Laboratory to study the effect of gradation and hydrograph on pier local scour. This chapter briefly describes the flume, the individual measurements, the sediment mixtures, and the description of the operational procedures.

4.1 The flume.

For the experiments a 60 ft long, 2 ft wide, and 4 ft deep flume was used. The flume is a recirculating tilting type, the bed slope can be adjusted by a screw jack at the downstream end as shown in Fig. 4.1 (El-Gamal 1991). The side walls along the entire length of the flume are constructed of 1/2 inch plexiglass. Water is pumped from a sump tank by a 20-hp pump through a 12 inch pipeline to the head box where a box of gravel was placed to reduce the turbulence at the flume entrance. A bottom hinged, adjustable, inclined steel gate is installed at the downstream end of the flume to control the water depth. An instrument carriage runs longitudinally along the flume rails, and laterally as well. A point gage with an accuracy of 0.001 ft is mounted on the instrument carriage. Measurements were taken at fifteen different sections along the flume including a section just upstream of each pier.

A 4 inch false floor, 2 ft wide, 36 ft long is placed in the middle portion of the flume with a gentle reversed slope of 1:4 at the upstream end. At the downstream end

of the false floor, a crest 2 ft wide, 2 inch long, and 6 inch high is placed to create a drop of 10 inches on its downstream. Three plexiglass piers of diameters 2.0, 2.0 and 2.75 inches were installed in the flume, equidistant from the walls. Fig. 4.1 shows piers locations along the flume.

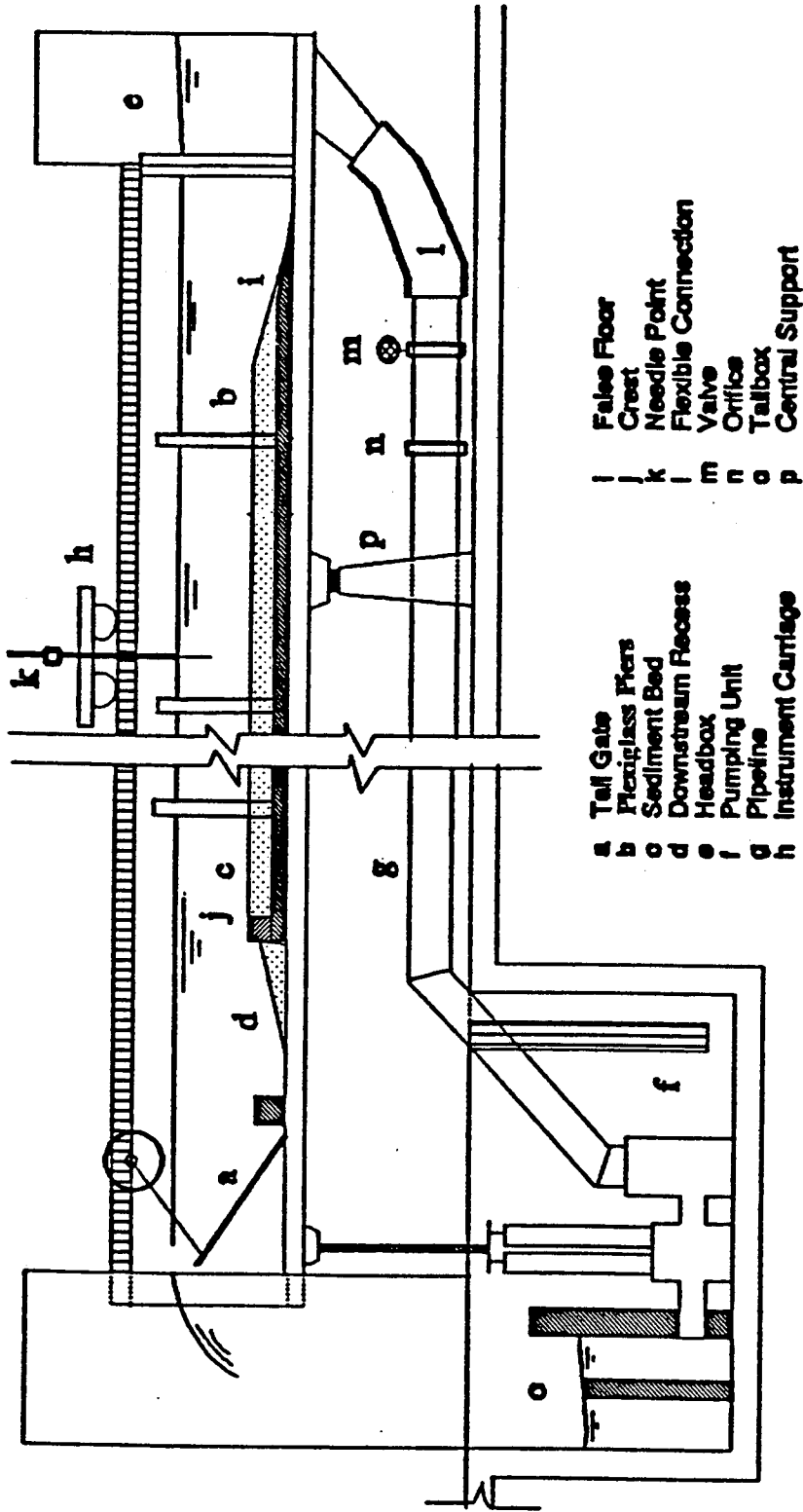


Figure (4.1) Schematic Diagram for the 2.0 ft flume

4.2 Individual measurements.

4.2.1 Discharge.

The discharge was measured on a water manometer by reading the difference in pressure head upstream and downstream of a calibrated segmental orifice meter mounted on the main pipeline. The manometer was calibrated and the discharge is already expressed as a function of the difference in pressure head, H , as $Q=0.077(H)^{1/2}$. The discharge can be regulated by the use of a valve in the main pipeline.

4.2.2 Flow depth.

The bed surface was levelled using a flat plexiglass plate with the same width as the flume connected vertically to the instrument carriage by clamps. The bottom edge of the flat plate was adjusted to the required elevation of the bed surface, and the carriage was then pushed by hand carefully and slowly to produce a smooth plane surface with the required thickness over the entire length of the sediment bed. At each section of the fifteen sections along the flume, ten different point gage bed readings was taken across the width of the flume. The actual bed reading was then considered to be the average of the ten readings. This technique was used to reduce the effect of bed irregularities, especially in the nonuniform material, on the accuracy of measurements of bed readings. The corresponding water surface readings at every section were taken at four points, and the actual water surface was considered to be the average of the four readings. The flow depth was calculated as the difference between the bed surface and water surface average readings at the specified section. The flow depth of the flow is measured from the top of the grains to the water surface.

4.2.3 Slope.

Slope has always been one of the most difficult quantities to measure and because of the one-to-one dependency of the determination of each pier's approaching shear stress and the measured slope, it was important to reduce the error in the measured slope. With the point gage readings of the bed surface and water surface determined as in the procedure mentioned in 4.2.2, the bed and water surface elevations were determined to a fixed point. The bed and water surface slope was then calculated through a least-square analysis as the slope of the line of best fit.

4.3 Sediment mixture.

Four different sediment mixtures following the log normal size distribution were used in the experiments. Such type of size distribution can be represented by a straight line on logarithmic-probability paper and in this case D_{50} becomes the geometric mean diameter, D_g , of the sediment mixture and the geometric standard deviation, σ_g , is given by the formula:

$$\sigma_g = \frac{D_{84}}{D_{50}} = \frac{D_{50}}{D_{16}} \quad (4.1)$$

or

$$\sigma_g = \sqrt{\frac{D_{84}}{D_{16}}} \quad (4.2)$$

where D_{16} , D_{50} , and D_{84} are the sediment diameter for which 16, 50, and 84 percentage by weight of the sediment material is finer.

Two of the four mixtures were required to be uniform while the other two were required to have different values for the geometric standard deviation. After the geometric mean diameter and the geometric standard deviation is chosen for a proposed mixture, the value of its D_{16} and D_{84} can be determined. The grain size distribution curve of the mixture can be drawn on logarithmic-probability paper as a straight line passing through D_{16} , D_{50} , and D_{84} so that the percentage of retained weight and consequently the required weight of each fraction could be easily calculated. The sediment material was brought in bulk quantities and sieved into the required fraction, according to the proposed grain size distribution, using a series of sieves and a mechanical shaker. Each obtained fraction of the sieved sediment material was stored in separate plastic bags. The sieving of the material was carried out until sufficient quantities of the required fraction was obtained. Batching of the sediment mixture to its correct grading was done through 20 kilogram batches by careful weighing of the required weight of each fraction and mixing manually in a wide container.

For the proposed uniform mixtures the sieving of the material was carried out using only two sieve sizes, slightly smaller and larger than the required geometric mean diameter. The mixture was obtained by collecting the material that is passing through the larger sieve size and retained on the smaller sieve size.

Table 4.1 indicate the used grain size distributions of the four sediment mixtures, also Fig. 4.2 shows their grain size distribution curves.

Table (4.1) Grain Size Distribution for Sediment Mixtures

SIEVE DIAMETER (mm)	MIXTURE (1)	MIXTURE (2)	MIXTURE (3)	MIXTURE (4)
10	100	100	100	100
8	94.9	100	100	100
6.68	92.35	100	100	100
5.6	85.32	100	100	100
4.76	80.28	100	93.6	100
4	73.68	100		100
2.83	60.1	100		100
2.38	56.3	100	62.5	100
2	51.62	65	55	100
1.65	47.13	24	46.2	
1.4	42.64	2.4		99.94
1.19	38.82	0.24	31.4	99.31
1	34.53	0	0	82
0.83	30.18	0	0	61.89
0.6	22.28	0	0	
0.5	20.99	0	0	3.73
0.42	18.84	0	0	1.24
0.3	12.42	0	0	0.93
0.13	0.91	0	0	
0.09	0.03	0	0	0
SIGMA	3.7	2.17	1.15	1.28

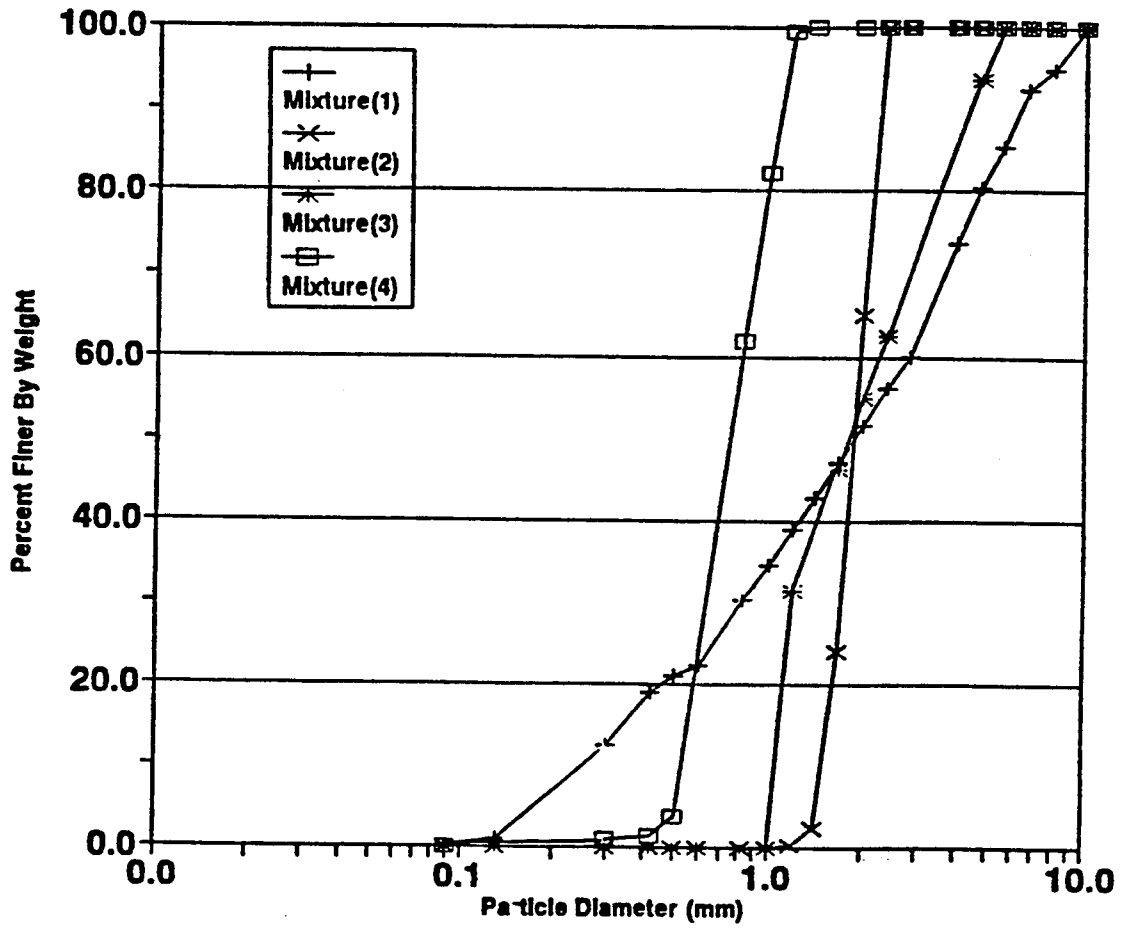


Figure (4.2) Gradation Curves for Sediment Mixtures

4.4 Description of testing procedure.

The main objective of the experimental work was to study the local scour around the cylindrical piers for the different bed sediment mixtures. Before starting the experiment the initial bed slope and bed levels around the piers were measured. The water was then pumped into the flume at a very low rate until a pool was formed in the upstream reach of the flume between the head box and the upstream end of the false floor. This filling process allowed the sediment bed to be wetted very slowly without causing any disturbance to the bed surface, especially around the piers. The discharge then was increased gradually with the gate adjusted as close as possible to the vertical position so as to maintain a large flow depth. The large flow depth existing while reaching the required discharge, made it possible to avoid any kind of bed surface disturbance around the piers. After reaching the required discharge the downstream gate was gradually adjusted to reach the desired preselected depth of flow. Then the discharge and the flow depth were held constant during the entire experiment time.

The objective of the experimental work was also to compare the local scour of simulated hydrographs to that of a steady flow. Two different sets of runs were carried out for each bed sediment mixture. The runs for steady flows were continued for a sufficiently long time, namely, up to 30 hrs till the equilibrium scour depth was attained. Unsteady flow, the hydrograph simulation, was obtained by regulating the main pipeline valve to attain equal discharge steps. During each unsteady flow run, six such steps were used to reach the required peak flow, with the gate fixed so as to maintain the flow depth for the peak discharge same as it was in case of the steady flow. Therefore, the

hydrograph discharge is discretized into different segments in which the flow is assumed to be steady, as shown in Fig. 4.3. Different values of time steps, Δt , were used for discretization, namely 2.5, 5.0, and 7.5 minutes, for two different discharge peaks 0.487 and 0.73 cfs.

A flash flood simulation was also conducted, where the discharge peak was attained in 1.5 minutes. The discharge peak was kept for 2.5 minutes.

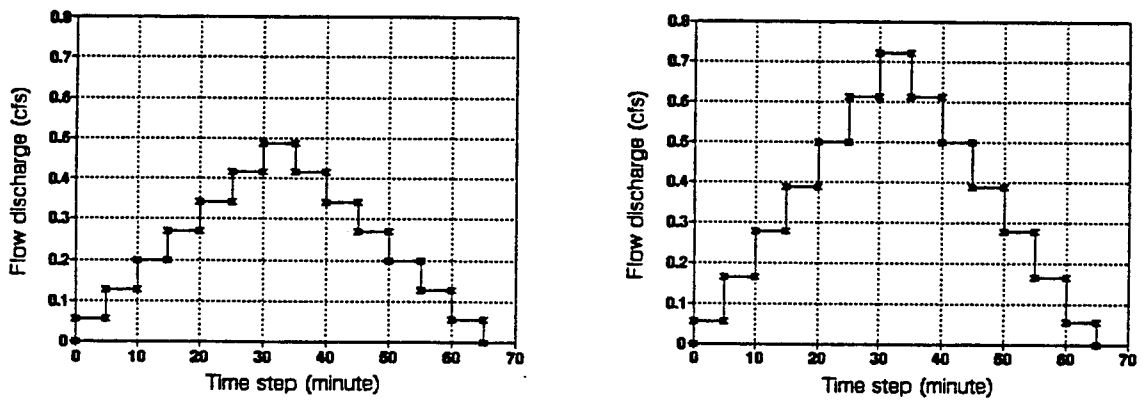


Fig. 4.3 The 5.0 minute discretized hydrograph for the two different peaks

For each steady flow run, each pier's approaching velocities were measured along the flow depth one foot upstream the pier. At least ten measurements of velocities were then taken for each vertical. Velocities were measured using a Marsh-McBirney 2-D magnetic velocity meter, attached to the point gage to read values in two orthogonal directions in a plane parallel to the bottom of the flume. As the velocity fluctuates near the pier and the velocity meter only gave measurements averaged at most over a period of 5 seconds, it was necessary to utilize a more complex setup of devices to measure a higher number of values averaged over a longer period of time to obtain more accurate values for the approaching velocity. For this purpose, the current meter was connected to an AC to DC data acquisition board which, in its turn, was connected to an IBM personal computer. A software, LASER, that was developed in Colorado State University by Dr. Albert Molinas and Nagi G. Reiad, read, stored, and averaged the velocity measurements over a period of 30 seconds at a sampling frequency of 50 Hz.

After each run the bed was let to dry and then measurements were taken for the bed elevations, maximum scour, and scour hole contours. Using paste, bed samples were taken for the scour hole surface material, the deposition surface material downstream the pier, and the approaching bed surface material.

The discharge was then increased slightly in successive runs for the same sediment mixture and the same procedures were repeated. The values of maximum discharges were chosen in such a way to have the corresponding shear stress values in the undisturbed flow below the critical values for beginning of motion. This allowed to maintain clear water scour conditions in all runs.

CHAPTER V.

RESULTS AND DISCUSSION OF RESULTS.

The following measured parameters, for each experiment, were available for the analysis: the grain size distribution of the mixture, the water discharge, Q , each pier approaching velocity, U , the approaching water depth, Y_1 , the bed slope, S_o , grain size distribution of the bed and the scour hole, and of course the maximum scour depth.

5.1 Scour in steady (long duration) flow.

This section describes the observed and experimental results of 20 runs of four different bed material mixtures of mean diameters, D_{50} , of 1.87, 1.80 and 0.76 mm. Details of measurements and procedures are given in Chapter IV.

5.1.1 Contraction scour.

It was observed in all the runs, through the comparison of the bed surface before and after each run, that there was not any contraction scour. According to (Richardson, 1989), the contraction scour should be negligible if the contraction of the channel is less than 10 percent. The presence of the piers resulted in contraction of 8.3, 8.3, and 11.46 percent of the width. The measurements verified the suggestion provided by Richardson.

5.1.2 Local pier scour.

Through dimensional analysis Melville and Sutherland (1988) showed that the

relative scour depth around piers is related to different dimensionless groups as follows

$$\frac{Y_s}{b} = (Fr, \frac{Y_1}{b}, \frac{D_{50}}{b}, \sigma_s, Sh, Al) \quad (5.1)$$

where Sh and Al are parameters describing the shape and alignment of the pier, and they are canceled in case of circular piers.

Regression analysis was used to develop an equation for local clear water scour around circular piers as a function of these dimensionless groups. The measured values of Y_s/Y_1 were regressed against every combination of the dimensionless groups. Different types of linear, polynomial, and power equations were tried with the different dimensionless groups. A computer software, MINITAB, was used in the regression analysis. The theory of this program is based on the least square methods.

5.1.2.1 Maximum local scour for uniform material.

The measured values of Y_s/Y_1 of 10 runs using the uniform mixtures (2) and (4) having mean diameter of 1.87 and 0.76 respectively, were regressed against every combination of the dimensionless groups. The measured values of Y_s/Y_1 were found to be highly correlated to Froude number. The best fitting equation's output results from MINITAB program are presented in table 5.1 and Fig. 5.1.

The regression equation:

$$\frac{Y_s}{Y_1} = 6.18 Fr - 5.22 Fr^2 - 0.716 \quad (5.2)$$

The measured values of Y_s/Y_1 for each mixture were also regressed separately against every combination of the dimensionless groups. The best fitting equation's output results from MINITAB program are presented in tables 5.1 (a) and 5.1 (b) for mixtures (2) and (4) respectively.

The regression equations for mixture (2) ($D_{50}=1.87$ mm):

$$\frac{Y_s}{Y_1} = 3.47 Fr - 0.60 Fr^2 - 0.497 \quad (5.2) \text{ (a)}$$

The regression equations for mixture (4) ($D_{50}=0.76$ mm):

$$\frac{Y_s}{Y_1} = 10.75 Fr - 12.15 Fr^2 - 1.176 \quad (5.2) \text{ (b)}$$

Fig 5.1 shows the measured data and the fitted data using equations 5.2, 5.2 (a), and 5.2 (b).

The presented expression of Y_s/Y_1 in eq. 5.2 was found to be very close to Chitale's formula (1944) that was presented in Chapter 3, eq. 3.2. Chitale's formula was derived for clear water scour, Froude number ranging from 0.1 to 0.45, and sand diameter of 0.16 to 1.51, which is very similar to the conditions used in deriving eq. 5.2.

Table 5.1 The output of the regression equations
for uniform mixtures

Predictor	Coeff.	Standard Deviat. of Coeff.	T-ratio Coef./SD	P
Constant	-0.7164	0.2662	-2.69	0.012
Fr	6.181	1.977	3.13	0.004
Fr ²	-5.216	3.31	-1.58	0.127
S = 0.2214				
R-square = 67.6 %				
R-square = 65.2 %, adjusted for D.F.				

Analysis of Variance

Source	D.F.	SS	MS=SS/D	F
regression	2	2.7662	1.3831	28.22
residual	27	1.3234	0.049	
total	29	4.0896		
Source	D.F.	SEQ SS		
Fr	1	2.6445		
Fr ²	1	0.1217		

Ys/Y1	Fr	Fr ²	Ys/Y1	Fr	Fr ²
0.02033	0.188313	0.035462	0.208	0.20619	0.042512
1E-05	0.13768	0.018956	0.0346	0.14424	0.020804
1E-05	0.110271	0.01216	0.01553	0.12422	0.015432
0.0873	0.249247	0.062124	0.81452	0.2693	0.072521
1E-05	0.171956	0.029569	0.2847	0.1855	0.034412
1E-05	0.140902	0.019853	0.17834	0.15725	0.024726
0.6449	0.299067	0.089441	1.02692	0.2955	0.087318
0.10432	0.207225	0.042942	0.6431	0.20307	0.041239
0.14596	0.161491	0.026079	0.4697	0.17547	0.030791
0.74118	0.314083	0.098648	1.06923	0.33835	0.114481
0.14236	0.220014	0.048406	0.73064	0.27033	0.07308
0.16918	0.180722	0.03266	0.82727	0.20584	0.042372
0.99213	0.444078	0.197205	1.06667	0.52519	0.275828
0.47917	0.318528	0.10146	0.74227	0.36915	0.136272
0.17988	0.249241	0.062121	0.62382	0.29642	0.087862

D.F. = Degrees of freedom ; SS = Sum of squares of deviations

MS = Sum of squares/degrees of freedom

P = Probability of getting a value as extreme as large in magnitude from t-dist.

T = Coefficient of regression variable/standard deviation

Table 5.1 (a) The output of the regression equations
for uniform mixture $D_{50} = 1.87$ mm.

Predictor	Coeff.	Standard Deviat. of Coeff.	T-ratio Coef./SD	P
Constant	-0.4972	0.1924	-2.58	0.021
Fr	3.473	1.394	2.49	0.025
Fr ²	-0.603	2.25	-0.27	0.792
S = 0.1309				
R-square = 88.8 %				
R-square = 87.3 %, adjusted for D.F.				

Analysis of Variance

Source	D.F.	SS	MS=SS/DF	F
regression	2	2.0275	1.0138	59.19
residual	15	0.2569	0.0171	
total	17	2.2844		
Source	D.F.	SEQ SS		
Fr	1	2.0263		
Fr ²	1	0.0012		

Ys/Y1	Fr	Fr ²	Ys/Y1	Fr	Fr ²
0.02033	0.188313	0.035462	1.06667	0.52519	0.275828
1E-05	0.13768	0.018956	0.74227	0.36915	0.136272
1E-05	0.110271	0.01216	0.62382	0.29642	0.087862
0.0873	0.249247	0.062124			
1E-05	0.171956	0.029569			
1E-05	0.140902	0.019853			
0.6449	0.299067	0.089441			
0.10432	0.207225	0.042942			
0.14596	0.161491	0.026079			
0.74118	0.314083	0.098648			
0.14236	0.220014	0.048406			
0.16918	0.180722	0.03266			
0.99213	0.444078	0.197205			
0.47917	0.318528	0.10146			
0.17988	0.249241	0.062121			

D.F. = Degrees of freedom ; SS = Sum of squares of deviations
MS = Sum of squares/degrees of freedom
P = Probability of getting a value as extreme as large in magnitude from t-dist.
T = Coefficient of regression variable/standard deviation

Table 5.1 (b) The output of the regression equations
for uniform mixture $D_{50} = 0.76$ mm.

Predictor	Coeff.	Standard Deviat. of Coeff.	T-ratio Coef./SD	P
Constant	-1.1756	0.6647	-1.77	0.111
Fr	10.754	6.106	1.76	0.112
Fr ²	-12.15	13.19	-0.92	0.381
S = 0.1746				
R-square = 82.4 %				
R-square = 78.5 %, adjusted for D.F.				

Analysis of Variance

Source	D.F.	SS	MS=SS/DF	F
regression	2	1.28677	0.64338	21.11
residual	9	0.27428	0.03048	
total	11	1.56105		
Source	D.F.	SEQ SS		
Fr	1	1.2609		
Fr ²	1	0.02587		

Ys/Y1	Fr	Fr ²
0.208	0.206185	0.042512
0.0346	0.144237	0.020804
0.01553	0.124224	0.015432
0.81452	0.269297	0.072521
0.2847	0.185504	0.034412
0.17834	0.157245	0.024726
1.02692	0.295496	0.087318
0.6431	0.203074	0.041239
0.4697	0.175473	0.030791
1.06923	0.338351	0.114481
0.73064	0.270334	0.07308
0.82727	0.205844	0.042372

- D.F. = Degrees of freedom ; SS = Sum of squares of deviations
MS = Sum of squares/degrees of freedom
P = Probability of getting a value as extreme as large in magnitude from t-dist.
T = Coefficient of regression variable/standard deviation

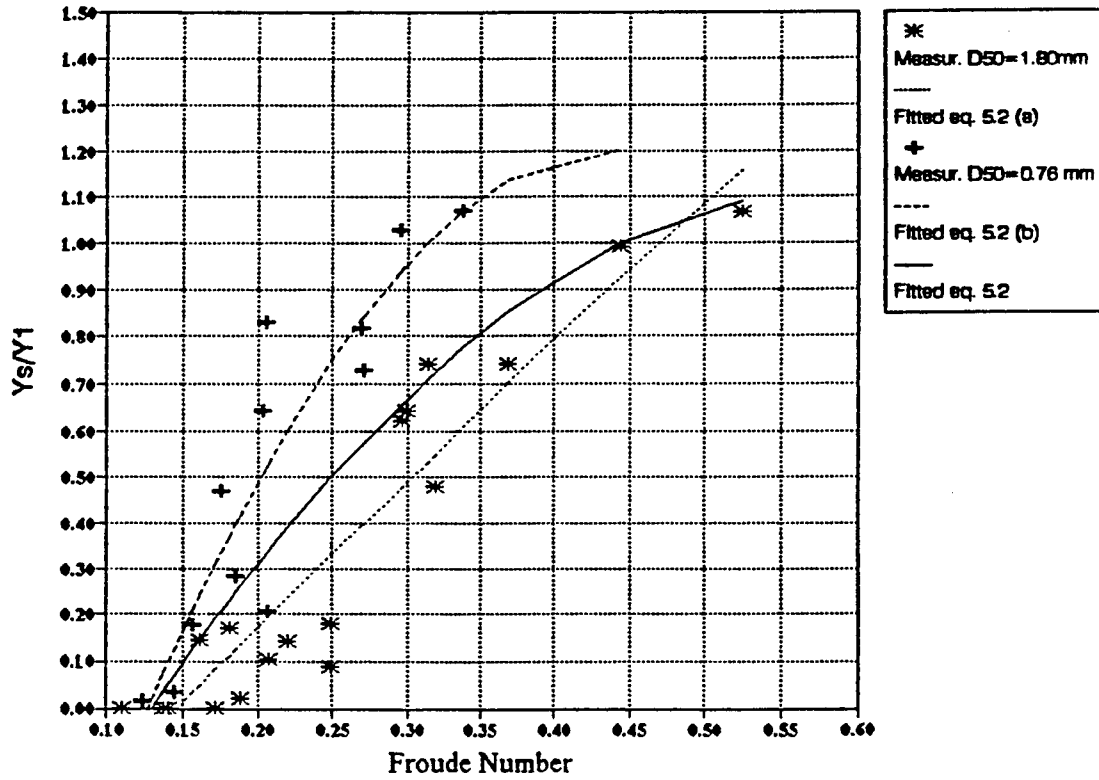


Fig. 5.1 Measured and fitted Y_s/Y_1 for uniform bed material.

5.1.2.2 Maximum local scour for highly graded material ($\sigma_g = 3.7$).

The measured values of Y_s/Y_1 of 5 runs using mixture (1) having mean diameter of 1.87, were regressed against every combination of the dimensionless groups. The measured values of Y_s/Y_1 were found to be highly correlated to Froude number. The best fitting equation's output results from MINITAB program are presented in table 5.2.

The regression equation:

$$\frac{Y_s}{Y_1} = - 0.03 Fr + 1.22 Fr^2 - 0.0176 \quad (5.3)$$

The measured and the fitted scour depth values for the highly graded bed material are shown in Fig. 5.2.

Table 5.2 The output of the regression equations
for mixture (1)

Predictor	Coeff.	Standard Deviat. of Coeff.	T-ratio Coef./SD	P
Constant	0.0176	0.2067	0.09	0.933
Fr	-0.03	1.079	-0.03	0.978
Fr ²	1.222	1.327	0.92	0.375
S = 0.0738				
R-square = 75.4 %				
R-square = 71.4 %, adjusted for D.F.				

Analysis of Variance

Source	D.F.	SS	MS=SS/D	F
regression	2	0.2008	0.1004	18.44
residual	12	0.06535	0.00545	
total	14	0.26615		
Source	D.F.	SEQ SS		
Fr	1	0.19619		
Fr ²	1	0.00462		

Ys/Y1	Fr	Fr ²
0.251908	0.331089	0.10962
0.054545	0.234274	0.054884
0.065217	0.193091	0.037284
0.378505	0.544755	0.296758
0.121339	0.414544	0.171847
0.159091	0.35327	0.1248
0.245833	0.457104	0.208944
0.106838	0.324231	0.105126
0.102881	0.27527	0.075774
0.379592	0.569651	0.324502
0.155039	0.4545	0.20657
0.172932	0.396359	0.1571
0.430894	0.607576	0.369149
0.341176	0.516492	0.266764
0.460937	0.480652	0.231026

D.F. = Degrees of freedom ; SS = Sum of squares of deviations

MS = Sum of squares/degrees of freedom

P = Probability of getting a value as extreme as large in magnitude from t-dist.

T = Coefficient of regression variable/standard deviation

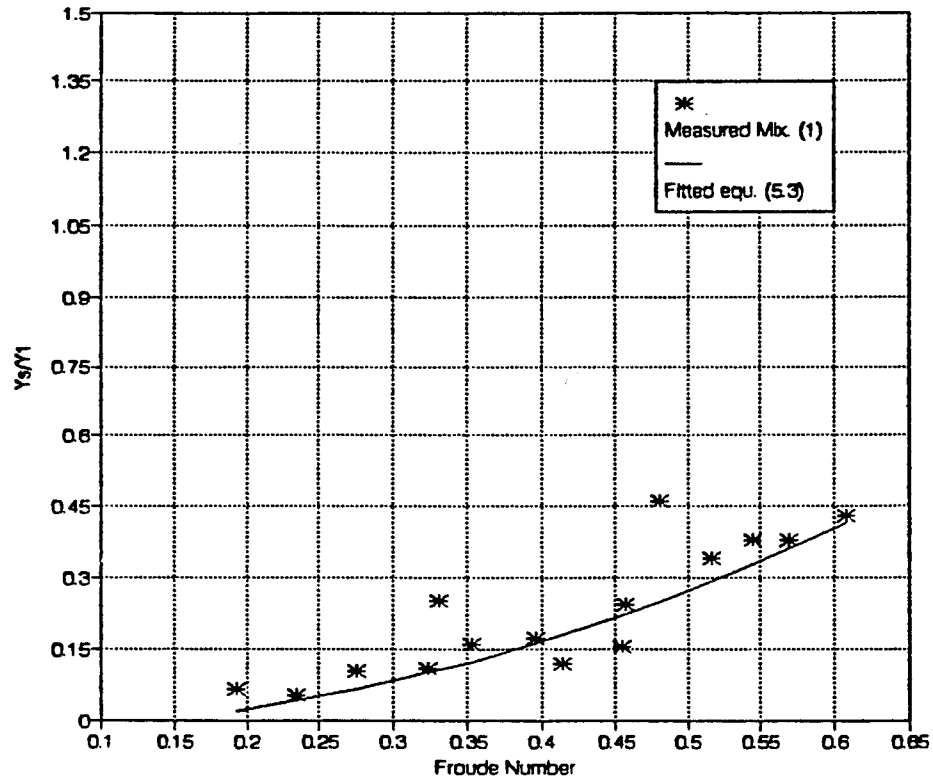


Fig. 5.2 Measured and fitted Y_s/Y_1 for highly graded mixture

5.1.2.3 Maximum local scour for moderately graded material ($\sigma_g = 2.17$).

The measured values of Y_s/Y_1 of 4 runs using mixture (3) having mean diameter of 1.80, were regressed against every combination of the dimensionless groups. The measured values of Y_s/Y_1 were found to be highly correlated to Froude number. The best fitting equation's output results from MINITAB program are presented in table 5.3.

The regression equation:

$$\frac{Y_s}{Y_1} = - 0.59 Fr + 4.10 Fr^2 + 0.04 \quad (5.4)$$

The measured and the fitted scour depth values for the moderately graded bed material are shown in Fig. 5.3.

It was noticed that the coefficients of Fr and Fr^2 for the uniform bed material, eq. 5.2, and the same coefficients for the graded bed material, eq. 5.3 and 5.4, have reversed signs. The reversed signs are attributed to the effect of bed material gradation.

Table 5.3 The output of the regression equations for mixture (3).

Predictor	Coeff.	Standard Deviat. of Coeff.	T-ratio Coef./SD	P
Constant	0.0398	0.2079	0.19	0.853
Fr	-0.59	1.454	-0.41	0.694
Fr ²	4.102	2.398	1.71	0.121
S = 0.05784				
R-square = 91.2 %				
R-square = 89.2 %, adjusted for D.F.				

Analysis of Variance

Source	D.F.	SS	MS=SS/D	F
regression	2	0.31217	0.15609	46.65
residual	9	0.03011	0.00335	
total	11	0.34228		
Source	D.F.	SEQ SS		
Fr	1	0.30238		
Fr ²	1	0.00979		

Ys/Y1	Fr	Fr ²
0.146429	0.231461	0.053574
0.03367	0.200487	0.040195
0.068966	0.152888	0.023375
0.165493	0.295962	0.087594
0.132258	0.253527	0.064276
0.129338	0.218473	0.04773
0.352941	0.367804	0.13528
0.222973	0.317757	0.10097
0.205128	0.267541	0.071578
0.541379	0.440472	0.194016
0.489437	0.409387	0.167598
0.496711	0.36277	0.131602

D.F. = Degrees of freedom ; SS = Sum of squares of deviations

MS = Sum of squares/degrees of freedom

P = Probability of getting a value as extreme as large in magnitude from t-dist.

T = Coefficient of regression variable/standard deviation

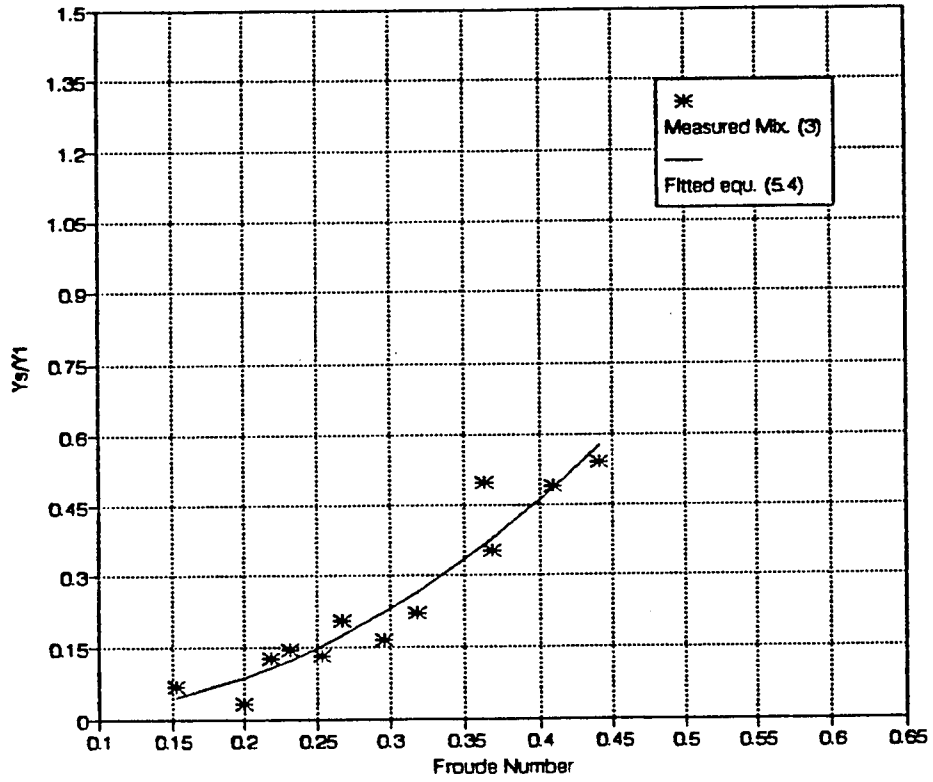


Fig. 5.3 Measured and fitted values for moderately graded mixture.

5.1.3 The coefficient of gradation K_g .

The coefficient K_g is a coefficient to relate the maximum expected local scour depth of the uniform and the graded bed material. It was computed from the fitted values of Y_s/Y_1 for the uniform and the graded bed material mixtures for every measured Froude number by the following equation:

$$\left(\frac{Y_s}{Y_1}\right)_{graded} = K_g \left(\frac{Y_s}{Y_1}\right)_{uniform} \quad (5.5)$$

The values K_g were found to be highly correlated to the geometric standard deviation of the particle size distribution and Froude number. The best fitting equation's output results from MINITAB program are presented in table 5.4.

The regression equation:

$$K_g = 2.82 \sigma_g^{-1.33} Fr^{0.849} \quad (5.6)$$

The equation is tested for $2.0 \leq \sigma_g \leq 4.0$. A comparison between K_g presented by Raudkivi and Ettema (1986) and that presented in equation 5.6 is shown in Fig. 5.4. A series of curves for determination of the coefficient of gradation are also shown in Fig. 5.5.

Table 5.4 The output of the regression equations
for the determination of Kg

Predictor	Coef.	Standard Deviat. of Coef.	T-ratio Coef./SD	P
Constant	0.45042	0.04595	9.8	0
Log(Sigma)	-1.32514	0.05571	-23.78	0
Log(Fr)	0.84896	0.06048	14.04	0
S = 0.02705				
R-square = 96.8 %				
R-square = 96.5 %, adjusted for D.F.				

Analysis of Variance

Source	D.F.	SS	MS=SS/DF	F
regression	2	0.42514	0.21257	290.57
residual	19	0.0139	0.00073	
total	21	0.43904		
Source	D.F.	SEQ SS		
Log(Sigma)	1	0.28101		
Log(Fr)	1	0.14413		

Kg	Sigma	Fr	Kg	Sigma	Fr
0.2814	2.17	0.228224	0.442556	2.17	0.36702
0.281903	2.17	0.229209	0.475007	2.17	0.386276
0.174399	3.7	0.236843	0.218806	3.7	0.400544
0.293109	2.17	0.246472	0.219205	3.7	0.401263
0.172672	3.7	0.268715	0.22075	3.7	0.404027
0.319419	2.17	0.275396	0.225416	3.7	0.412157
0.322644	2.17	0.278466	0.549594	2.17	0.426026
0.182206	3.7	0.316224	0.24553	3.7	0.444099
0.405286	2.17	0.343024	0.257543	3.7	0.461242
0.201308	3.7	0.365967	0.2765	3.7	0.486001
0.441773	2.17	0.366538	0.279826	3.7	0.490092

D.F. = Degrees of freedom; SS = Sum of squares of deviations

MS = Sum of squares/degrees of freedom

P = Probability of getting a value as extreme as large in magnitude from t-dist

T = Coefficient of regression variable/standard deviation

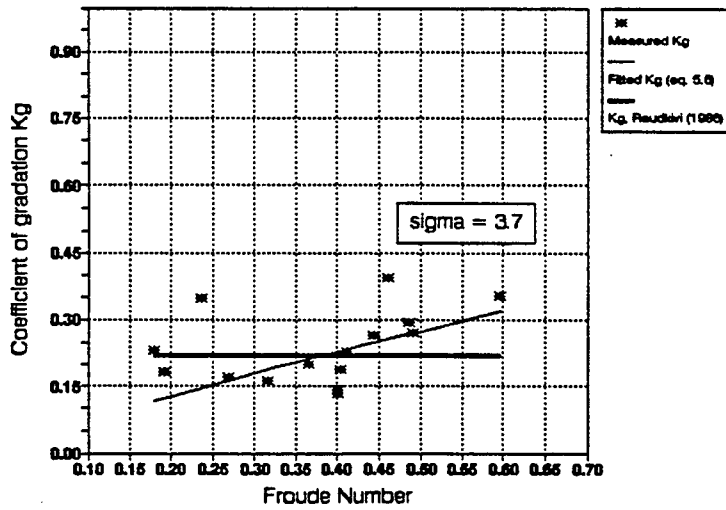
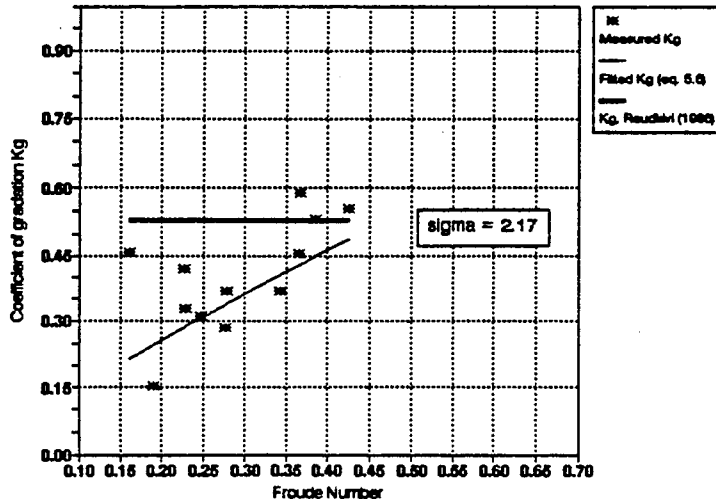


Fig. 5.4 Comparison between Kg of Raudkivi (1986) and eq. 5.6

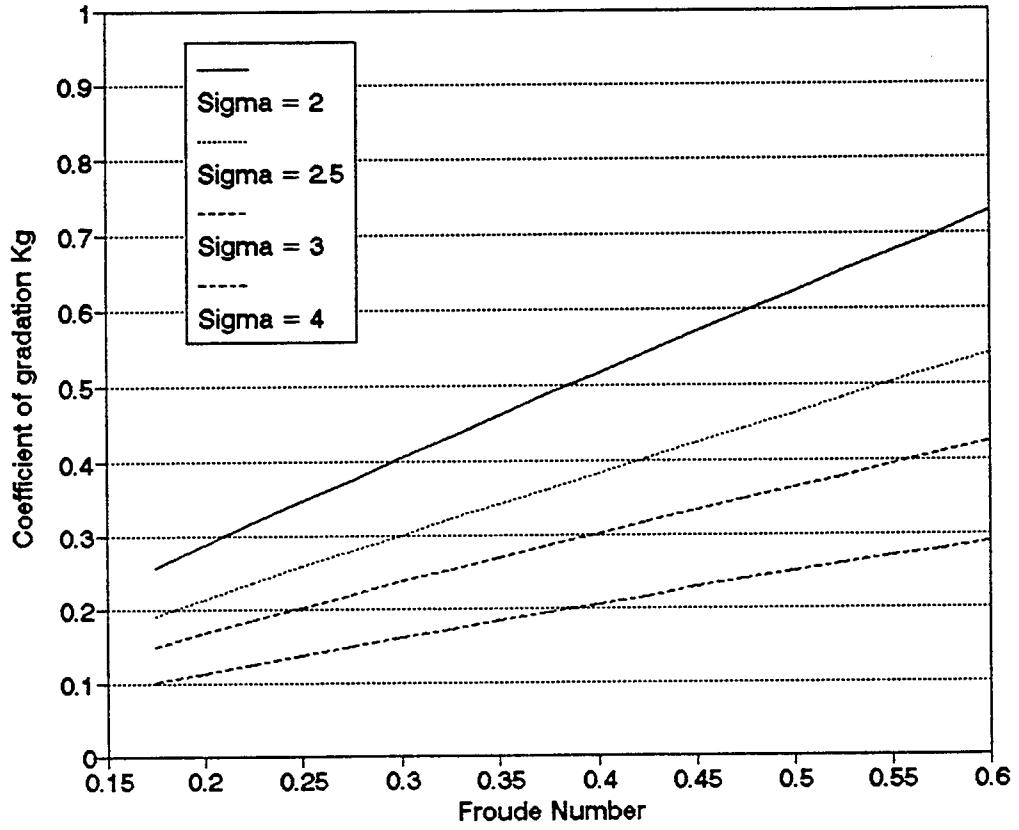


Fig. 5.5 The coefficient of gradation values from eq. 5.6.

5.2 Scour in unsteady flow (discretized hydrograph).

The hydrograph of flow was discretized into different segment in which the flow is assumed to be steady. Three different values of Δt (2.5, 5.0, 7.5 min.) were used in the discretization. The measured values of Y_s/Y_1 using 5.0 minute discretization for the four mixtures were regressed against every combination of the dimensionless groups and the measured values of Y_s/Y_1 for the corresponding steady flows with the exact same hydraulic conditions. The measured values of Y_s/Y_1 for the steady and unsteady flow were found to be highly correlated. The best fitted relation between the relative local scour depth around bridge piers for steady and the 5.0 minute discretized hydrograph can be expressed as follows:

The regression equation:

$$\left(\frac{Y_s}{Y_1}\right)_{5\text{min. Hyd.}} = 0.40 \left(\frac{Y_s}{Y_1}\right)^{2.44} \sigma_g^{1.58} \quad (5.7)$$

The best fitting equation's output results from MINITAB program are presented in table 5.5. The measured and the fitted values for the 5.0 minute discretized hydrograph are shown in Fig. 5.6.

Table 5.5 The output of the regression equations for the determination of the relation between the steady and the 5 min. peak flow

Predictor	Coeff.	Standard Deviat. of Coef.	T-ratio Coef./SD	P
Constant	-0.39553	0.09591	-4.12	0.003
Log(Ys/Y1)	2.4357	0.2583	9.43	0
Log(sigma)	1.5759	0.2597	6.07	0
S = 0.1723				
R-square = 91.7 %				
R-square = 89.8 %, adjusted for D.F.				

Analysis of Variance

Source	D.F.	SS	MS=SS/DF	F
regression	2	2.9447	1.4724	49.6
residual	9	0.2672	0.0297	
total	11	3.2119		
Source	D.F.	SEQ SS		
Log(Ys/Y1)	1	1.8518		
Log(sigma)	1	1.0929		

Ys/Y1 Hydr.	Ys/Y1	sigma	Log(Hydr)	LogYs/Y	Log(sigma)
0.317073	0.43089	3.7	-0.49884	-0.3656	0.568202
0.392157	0.34118	3.7	-0.40654	-0.467	0.568202
0.285156	0.46094	3.7	-0.54492	-0.3364	0.568202
0.429134	0.99213	1.15	-0.36741	-0.0034	0.060698
0.086806	0.47917	1.15	-1.06145	-0.3195	0.060698
0.006098	0.17988	1.15	-2.21481	-0.745	0.060698
0.27931	0.54138	2.17	-0.55391	-0.2665	0.33646
0.288732	0.48944	2.17	-0.53951	-0.3103	0.33646
0.338816	0.49671	2.17	-0.47004	-0.3039	0.33646
0.684615	1.06923	1.28	-0.16455	0.02907	0.10721
0.515152	0.73064	1.28	-0.28806	-0.1363	0.10721
0.239394	0.82727	1.28	-0.62089	-0.0824	0.10721

D.F. = Degrees of freedom; SS = Sum of squares of deviations

MS = Sum of squares/degrees of freedom

P = Probability of getting a value as extreme as large in magnitude from t-dist.

T = Coefficient of regression variable/standard deviation

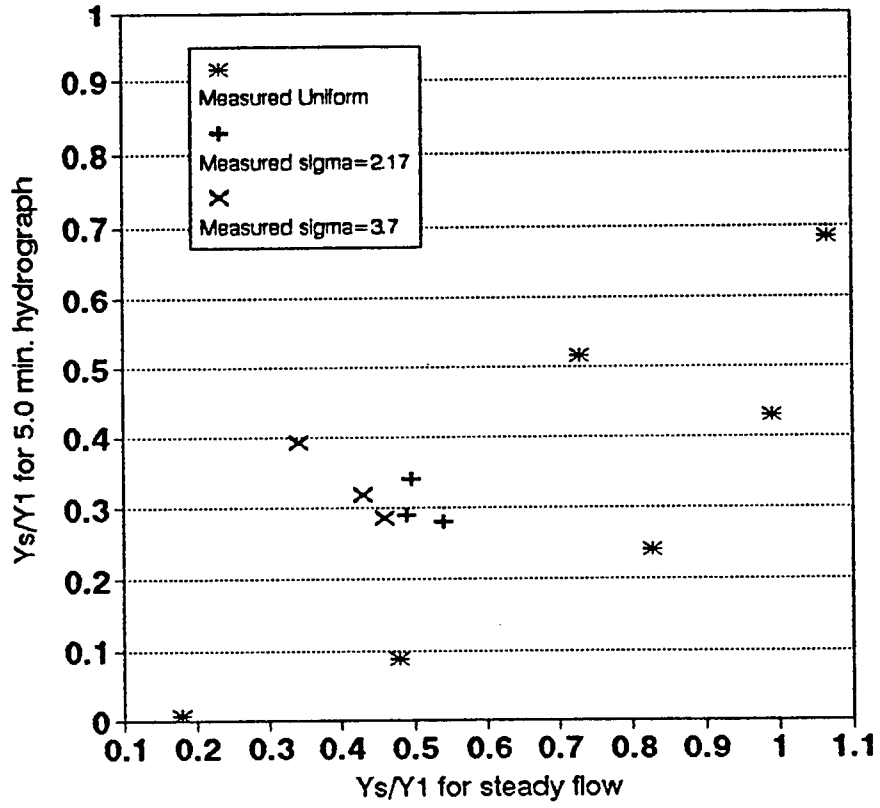


Fig. 5.6 The measured and fitted values for the 5.0 min. hydrograph

The measured values of Y_s/Y_1 using 2.5 and 7.5 minute discretization for the four mixtures were also found to be directly related to values of Y_s/Y_1 using the 5.0 minute discretization. The best fitted relative local scour depth around bridge piers for the case of 2.5 and 7.5 minute discretization can be expressed as a function of the 5.0 minute discretized hydrograph as follows:

The regression equation:

$$\left(\frac{Y_s}{Y_1}\right)_{2.5\text{min. Hyd.}} = 0.0459 + 0.79 \left(\frac{Y_s}{Y_1}\right)_{5\text{min. Hyd.}} \quad (5.8)$$

$$\left(\frac{Y_s}{Y_1}\right)_{7.5\text{min. Hyd.}} = 1.67 \left(\frac{Y_s}{Y_1}\right)_{5\text{min. Hyd.}}^{1.41} \quad (5.9)$$

The best fitting equations' output results from MINITAB program are presented in table 5.6 and 5.7.

The measured and the fitted scour depth values for the 2.5 and 7.5 minute discretization as a function of the 5.0 minute discretization measured values are shown in Fig. 5.7.

Table 5.6 The output of the regression equations for the relation between the 2.5 and 5 min. peak flows.

Predictor	Coeff.	Standard Deviat. of Coef.	T-ratio Coef./SD	P
Constant	0.04589	0.02178	2.11	0.061
(Ys/Y1)5 min.	0.79006	0.05973	13.23	0
S = 0.03542				
R-square = 94.6 %				
R-square = 94.1 %, adjusted for D.F.				

Analysis of Variance

Source	D.F.	SS	MS=SS/DF	F
regression	1	0.21954	0.21954	174.95
residual	10	0.01255	0.00125	
total	11	0.23209		

(Ys/Y1)2.5	(Ys/Y1) 5
0.308943	0.317073
0.282353	0.392157
0.308594	0.285156
0.433071	0.429134
0.090278	0.086806
0.064024	0.006098
0.282759	0.27931
0.239437	0.288732
0.338816	0.338816
0.592308	0.684615
0.434343	0.515152
0.227273	0.239394

D.F. = Degrees of freedom ; SS = Sum of squares of deviations

MS = Sum of squares/degrees of freedom

P = Probability of getting a value as extreme as large in magnitude from t-dist.

T = Coefficient of regression variable/standard deviation

Table 5.7 The output of the regression equations for the relation between the 7.5 and 5 min. peak flows.

Predictor	Coeff.	Standard Deviat. of Coef.	T-ratio Coef./SD	P
Constant	0.2221	0.1024	2.17	0.067
LogYs/Y1 5 m.	1.4078	0.1108	12.71	0
S = 0.1844				
R-square = 95.8 %				
R-square = 95.3 %, adjusted for D.F.				

Analysis of Variance

Source	D.F.	SS	MS=SS/DF	F
regression	1	5.4944	5.4944	161.5
residual	7	0.2381	0.034	
total	8	5.7325		

LogYs/Y1 7.5 min.	Ys/Y1 5.0 min.	LogYs/Y1 7.5 min	Log Ys/Y1 5.0 min.
0.394309	0.317073	-0.40416	-0.49884
0.192157	0.392157	-0.71634	-0.40654
0.316406	0.285156	-0.49976	-0.54492
0.413386	0.429134	-0.38364	-0.36741
0.086806	0.086806	-1.06145	-1.06145
0.001	0.006098	-3	-2.21481
0.358621	0.27931	-0.44536	-0.55391
0.401408	0.288732	-0.39641	-0.53951
0.342105	0.338816	-0.46584	-0.47004

D.F. = Degrees of freedom ; SS = Sum of squares of deviations

MS = Sum of squares/degrees of freedom

P = Probability of getting a value as extreme as large in magnitude from t-dist.

T = Coefficient of regression variable/standard deviation

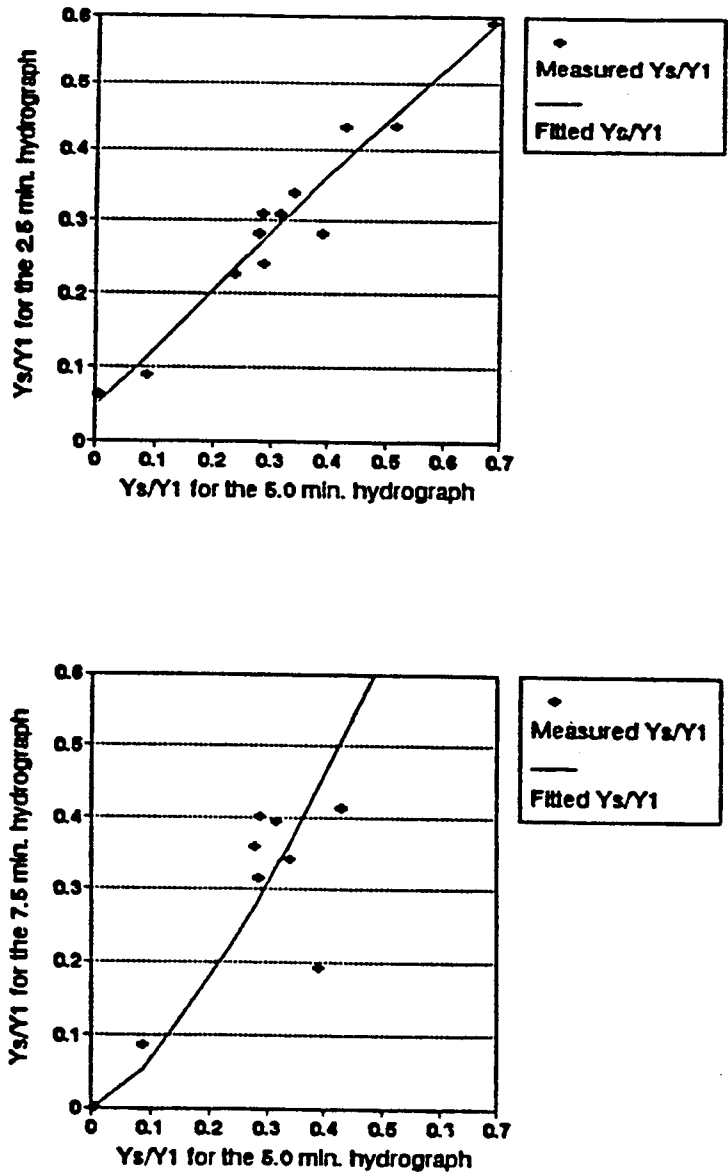


Fig. 5.7 The relation between the 2.5, 5.0, and 7.5 min. hydrographs.

In an attempt to investigate the effect of the time taken to reach the peak discharge on scour depth, the measured values of Y_s/Y_1 for the 2.5 minute hydrograph and the flash flood of the same peak were examined. The duration of the peak discharge in both tests were 2.5 minutes, but the time taken to reach the peak discharge was 30 minutes for the hydrograph and 1.5 minutes for the flash flood. The values of Y_s/Y_1 for the flash flood was generally slightly higher than that for the 2.5 minute hydrograph, although the time taken to reach the peak was longer for the hydrograph. The higher values of Y_s/Y_1 for the flash flood are attributed to the sweeping nature of the flood that is caused by the high discharge running with a very small flow depth in the beginning of the flood. The measured values of Y_s/Y_1 for the 2.5 minute hydrograph are plotted against their values for the flash flood in Fig. 5.8.

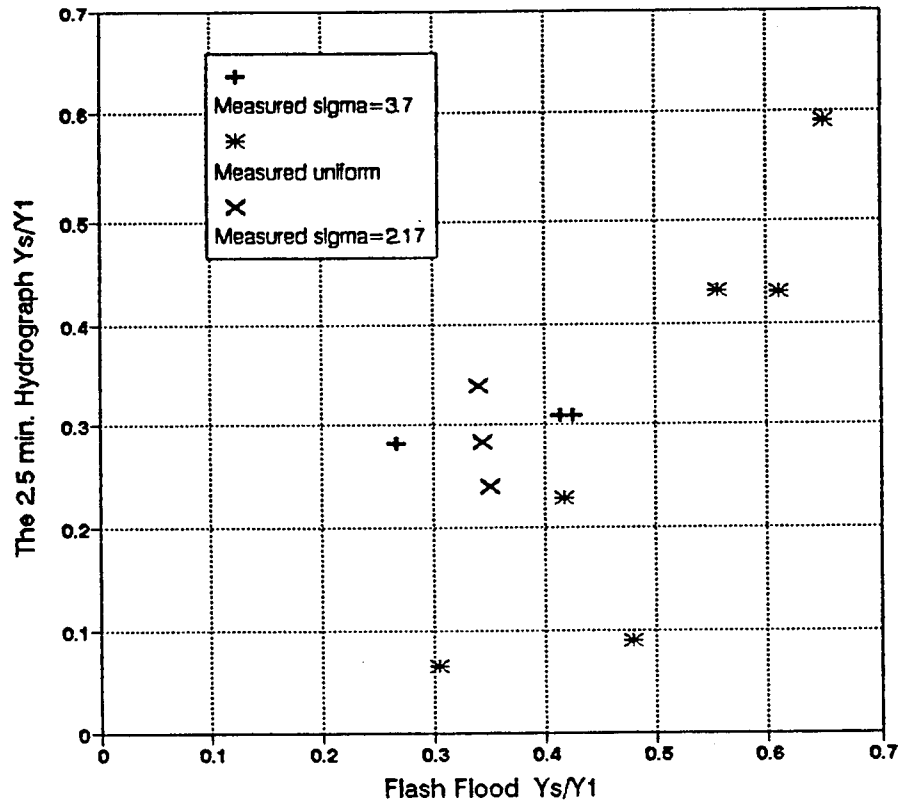


Fig. 5.8 Measured Y_s/Y_1 for the 2.5 min. hydrograph and the flash flood.

CHAPTER VI.

SUMMARY AND CONCLUSIONS.

6.1 Conclusive consideration.

In the last fifty years many prediction models were proposed for local scour around bridge piers. Many prediction models are presented (Chapter III) in a comprehensive literature review. The very complex nature of the problem makes the attempt of taking into the account all parameters very difficult. Nevertheless, the diverse parameters are of importance that must not be neglected. In particular, the scour prediction equations that do not consider the effect of sediment size and gradation should be modified. The gradation of the bed material considerably decreases the expected local scour depth than the case of a uniform bed having same mean diameter. The literature review revealed that the effect of gradation on clear water bridge pier scour was only studied by Raudkivi and Ettema (1983, 1986).

The literature review revealed also that the determination of the design scour depth is mainly based on use of relationships for maximum scour depth in steady long-duration flow along with the design discharge. Computations of Kothyari (1989) revealed that time taken by the design discharge to scour to its full potential is generally larger than the time for which it runs in real life. Therefore, hydraulic design of foundations based on computations of maximum scour depth for infinitely long design discharge can be too conservative.

A series of empirical relationships were developed through extensive experimentation to correlate the identifiable parameters from dimensional analysis of the local scour process at bridge pier for clear water scour. Uniform and graded bed material mixtures were used to study the effect of the gradation. The experiments also included simulated (discretized) hydrographs to study the relation between the maximum scour depth of the hydrograph and the steady long-duration flow. Three different time steps (2.5, 5.0, 7.5 min.) were used in discretizing the hydrographs. The experiments involved a series of thirty tests (fourteen tests in uniform bed material and sixteen tests in graded bed material). They were conducted in a tilting two foot flume at the Engineering Research Center of Colorado State University. The tests were performed using three circular piers of diameters 2.0, 2.0, and 2.75 inches. The ranges of flow depths were from 0.131 to 0.330 feet. Each of the steady tests was performed with constant discharge and Froude number ranged from 0.11 to 0.60. The results of the experimental data were used for a series of different considerations using dimensional and regression analysis.

1. A new equation (eq. 5.2) was developed for predicting the clear water local scour around circular bridge piers in uniform bed material. The maximum relative scour depth (Y_s/Y_1) is expressed as a function of Froude number. The equation was tested for Froude numbers up to 0.55 for mixtures with mean diameters of 1.87 mm. and 0.76 mm.
2. Two equations (eq. 5.3 and 5.4) were developed to predict the maximum clear water local scour around circular bridge piers for each of the two graded bed material mixtures with geometric standard deviations of 3.7 and 2.17.

3. Previous research by Raudkivi (1986) considered the effect of bed material gradation introducing a coefficient of gradation that only depends on the geometric standard deviation of particle size distribution. The data collected in the experiments of this thesis show, in fact, that the coefficient of gradation is strongly correlated to Froude number besides the geometric standard deviation. A new and more general expression for the coefficient of gradation (eq. 5.6) were introduced in this study. Hence, the predicted maximum clear water local scour around circular bridge piers in uniform or/and graded bed material, can be expressed as

$$\frac{Y_s}{Y_1} = K_g (6.18 Fr - 5.22 Fr^2 - 0.716) \quad (6.1)$$

in which K_g is not a constant, but a function of flow properties.

4. The maximum relative scour depth (Y_s/Y_1) of the 5.0 minute discretized hydrograph was found to be strongly related to the maximum relative scour depth of the steady flow. A new equation (eq. 5.7) was introduced in this study, relating the relative scour depth of the simulated hydrograph to that of the steady flow and geometric standard deviation of particle size distribution.

5. The characteristics of the relative scour depth of the different discretized hydrographs were examined in detail. The relative clear water scour depth of the 2.5 and 7.5 min. discretization were found to be highly related to that of the 5.0 min. discretization. Equations relating the relative scour depth of the different discretized hydrographs (eq. 5.8 and 5.9) were presented in this study.

6.2 Suggestions for further research.

1. All tests performed in this study were performed for the clear water scour case. It is suggested that similar study be performed with live bed scour case. The results of the two studies should be compared to determine the similarities of the two cases.
2. Throughout this study, the bed material was sand of median diameters 1.87, 1.8, and 0.76 mm. It is suggested that the discretized hydrograph tests should be performed with smaller, larger and cohesive bed material to test the effect of the size of bed material on the results introduced in this study.
3. It is suggested that scour experiments, similar to those described herein, be conducted with larger facilities. The results of the two studies should be compared.
4. More study should be pursued to the hydrograph discretization to be able to relate the experimental results to the natural hydrograph, to be able to use the results in the hydraulic design of bridge foundations.
5. It is suggested also that the scour caused by flash floods should be studied and compared with the maximum scour depth predicted by different models.

BIBLIOGRAPHY.

1. Baker, C.J., "New Design Equations for Scour around Bridge Piers", Journal of the Hydraulics Division, ASCE, Vol. 107, 1981, pp. 507-511.
2. Blaisdell, F.W., Anderson, C.L., Hebaus, G.G., "Ultimate Dimensions of Local Scour", Journal of the Hydraulics Division, ASCE, Vol. 1981, pp. 327-337.
3. Breusers, H.N.C., Nicollet, G., Shen, H.W., "Local Scour around Cylindrical Piers", Journal of Hydraulic Research, 1977, pp. 221-252.
4. Carstens, M.R., "Similarity Laws for Localized Scour", Journal of the Hydraulics Division, ASCE, 1966, Vol. 9.2, No.HY3, pp. 13-36.
5. Chiew, Y.M., "Scour Protection at Bridge Piers", Journal of Hydraulic Engineering, Vol. 118, 1992, pp. 1260-1269.
6. Dargahi, B., "Controlling Mechanism of Local Scouring", Journal of Hydraulic Engineering, Vol. 116, 1990, pp. 1197-1214.
7. El-Gamal, F.S., "Critical Shear Stress for Sediment Mixtures", Ph.D. dissertation, Colorado State University, Fort Collins, Colorado, Fall 1991.
8. Elliott, K.R., Baker, C.J., "Effect of Pier Spacing on Scour around Bridge Piers", Journal of Hydraulic Engineering, Vol.111, 1985, pp. 1105-1109.
9. Froehlich, D.C., "Analysis of Onsite Measurements of Scour at Piers", proceedings of ASCE National Hydraulic Engineering Conference, Colorado Springs, Colorado, pp. 534-539.
10. Jain, S.C., "Maximum Clear Water Scour around Circular Piers", Journal of Hydraulic Engineering, ASCE, Vol. 109, 1981, pp. 611-626.
11. Jain, S.C., Fisher, E.F., "Scour around Bridge Piers at High Flow Velocities", Journal of Hydraulic Engineering, ASCE, Vol. 104, 1980, pp. 1827-1842.
12. Johnson, P.A., "Reliability-Based Pier Scour Engineering", Journal of Hydraulic Engineering, Vol. 118, 1992, pp. 1344-1358.
13. Jones, J.S., Kilgore, R.T., Mistichelli, M.P., "Effects of Footing Location on Bridge Pier Scour", Journal of Hydraulic Engineering, Vol. 118, 1992, pp. 280-290.

14. Kothyari, U.C., Garde, R.J., Ranga Raju, K.G., "Live Bed Scour around Cylindrical Bridge Piers", *Journal of Hydraulic Research*, Vol. 30, 1992, pp. 701-714.
15. Kothyari, U.C., Garde, R.J., Ranga Raju, K.G., "Temporal Variation of Scour around Circular Bridge Piers", *Journal of Hydraulic Engineering*, Vol. 118, No. 8, 1992, pp. 1091-1106.
16. Laursen, E.M., "Observations on the Nature of Scour", proceedings 5th Hydraulics Conference, University of Iowa, Iowa, 1952, pp. 179-197.
17. Laursen, E.M., "Scour at Bridge Crossings", *Transactions ASCE*, Vol. 127, 1962, pp. 166-209.
18. Laursen, E.M., "Bridge Design Considering Scour an Risk", *Transportation Engineering Journal*, ASCE, 1970, pp. 149-164.
19. Laursen, E.M., "Assessing Vulnerability of Bridges to Floods", *Transportation Research Record*, Vol. 950, 1983, pp. 222-229.
20. Laursen, E.M., Toch, A., "Scour around Bridge Piers and Abutments", *Bulletin No. 4*, Iowa Highway Research Board, 1956.
21. Mellville, B.W., "Live Bed Scour at Bridge Piers", *Journal of Hydraulic Engineering*, ASCE, Vol. 110, 1984, pp. 1234-1247.
22. Mellville, B.W., Raudkivi, A.J., "Flow Characteristics in Local Scour at Bridge Piers", *Journal of the Hydraulic Research*, 1977, pp. 373-380.
23. Mellville, B.W., Sutherland, A.J., "Design Method for Local Scour at Bridge Piers", *Journal of the Hydraulic Engineering*, ASCE, Vol. 114, 1988, pp. 1210-1226.
24. Raudkivi, A.J., "Functional Trends of Scour at Bridge Piers", *Journal of Hydraulic Engineering*, ASCE, Vol. 112, 1986, pp. 1-13.
25. Raudkivi, A.J., Ettema, R., "Effect of Sediment Gradation on Clear Water Scour", *Journal of Hydraulics Division*, ASCE, Vol. 103, 1977, pp. 1209-1213.
26. Raudkivi, A.J., Ettema, R., "Clear Water Scour at Cylindrical Piers", *Journal of Hydraulic Engineering*, ASCE, Vol. 109, 1983, pp. 338-350.
27. Raudkivi, A.J., Ettema, R., "Scour at Cylindrical Bridge Piers in Armored Beds", *Journal of Hydraulic Engineering*, ASCE, Vol. 111, 1985, pp. 713-731.

28. Richardson, E.V., Simons, D., Julien, P.Y., "Highways in the River Environment", U.S. Department of Transportation, FHWA, 1987.
29. Shen, H.W., Schneider, V.R., Karaki, S., "Local Scour around Bridge Piers", Journal of the Hydraulics Division, ASCE, 1969, pp. 1919-1940.
30. Stevens, M.A., Gasser, M.M., Saad, M.B., "Wake Vortex Scour at Bridge Piers", Journal of Hydraulic Engineering, Vol. 117, 1991, pp. 891-904.
31. U.S. Department of Transportation, Federal Highway Administration, "Interim Procedures for Evaluating Scour at Bridges", 1988.
32. Yanmaz, A.M., Altinbilek, H.D., "Study of Time-Dependent Local Scour around Bridge Piers", Journal of Hydraulic Engineering, Vol. 117, 1991, pp. 1247-1268.

Appendix A
Data Summary of Pier Scour Experiments

RUN #	PARTICLE ST.DEVIAT.	SED.MEAN DIAM.(D50)	PIER DIAM.(b)	Q	APPR. DEPTH(Y1)	APPR. VELOCITY	FROUD NO.	BED SLOPE	DURA-TION	MAX SCR. DEPTH(Ys)
	(mm.)	(inch)	(cfs)	(inch)	(ft/sec)				(hrs.)	(inch)
R1P1	3.7	1.87	2	0.244	1.572	0.68	0.3311	0.00418	8	0.396
R1P2	3.7	1.87	2	0.244	1.98	0.54	0.2343	0.00418	8	0.108
R1P3	3.7	1.87	2.75	0.244	2.208	0.47	0.1931	0.00418	8	0.144
R2P1	3.7	1.87	2	0.487	2.568	1.43	0.5448	0.00418	8	0.972
R2P2	3.7	1.87	2	0.487	2.868	1.15	0.4145	0.00418	8	0.348
R2P3	3.7	1.87	2.75	0.487	3.168	1.03	0.3533	0.00418	8	0.504
R3P1	3.7	1.87	2	0.385	2.4	1.16	0.4571	0.003628	8	0.59
R3P2	3.7	1.87	2	0.385	2.808	0.89	0.3242	0.003628	8	0.3
R3P3	3.7	1.87	2.75	0.385	2.916	0.77	0.2753	0.003628	8	0.3
R4P1	3.7	1.87	2	0.621	2.94	1.6	0.5697	0.003357	10	1.116
R4P2	3.7	1.87	2	0.621	3.096	1.31	0.4545	0.003357	10	0.48
R4P3	3.7	1.87	2.75	0.621	3.192	1.16	0.3964	0.003357	10	0.552
R5P1	3.7	1.87	2	0.73	2.952	1.71	0.6076	0.003679	10	1.272
R5P2	3.7	1.87	2	0.73	3.06	1.48	0.5165	0.003679	10	1.044
R5P3	3.7	1.87	2.75	0.73	3.072	1.38	0.4807	0.003679	10	1.416
R6H1P1	3.7	1.87	2	0.73	2.952	1.71	0.6076	0.003679	F. FLOOD	1.224
R6H1P2	3.7	1.87	2	0.73	3.06	1.48	0.5165	0.003679	F. FLOOD	0.816
R6H1P3	3.7	1.87	2.75	0.73	3.072	1.38	0.4807	0.003679	F. FLOOD	1.308
R7H4P1	3.7	1.87	2	0.73	2.952	1.71	0.6076	0.003679	DT=2.5 M	0.912
R7H4P2	3.7	1.87	2	0.73	3.06	1.48	0.5165	0.003679	DT=2.5 M	0.864
R7H4P3	3.7	1.87	2.75	0.73	3.072	1.38	0.4807	0.003679	DT=2.5 M	0.948
R8H5P1	3.7	1.87	2	0.73	2.952	1.71	0.6076	0.003679	DT=5.0 M	0.936
R8H5P2	3.7	1.87	2	0.73	3.06	1.48	0.5165	0.003679	DT=5.0 M	1.2
R8H5P3	3.7	1.87	2.75	0.73	3.072	1.38	0.4807	0.003679	DT=5.0 M	0.876
R9H6P1	3.7	1.87	2	0.73	2.952	1.71	0.6076	0.003679	DT=7.5 M	1.164
R9H6P2	3.7	1.87	2	0.73	3.06	1.48	0.5165	0.003679	DT=7.5 M	0.588

RUN #	PARTICLE ST.DEVIAT.	SED.MEAN DIAM.(D50)	PIER DIAM.(b)	Q	APPR. DEPTH(Y1)	APPR. VELOCITY	FROUD NO.	BED SLOPE	DURA-TION	MAX SCR. DEPTH(Ys)
		(mm.)	(inch)	(cfs)	(inch)	(ft/sec)			(hrs.)	(inch)
R9H6P3	3.7	1.87	2.75	0.73	3.072	1.38	0.4807	0.003679	DT=7.5 M	0.972
R10P1	1.15	1.87	2	0.244	2.952	0.53	0.1883	0.00375	11	0.06
R10P2	1.15	1.87	2	0.244	3.468	0.42	0.1377	0.00375	11	0
R10P3	1.15	1.87	2.75	0.244	3.972	0.36	0.1103	0.00375	11	0
R11P1	1.15	1.87	2	0.318	3.024	0.71	0.2492	0.00375	9	0.264
R11P2	1.15	1.87	2	0.318	3.408	0.52	0.172	0.00375	9	0
R11P3	1.15	1.87	2.75	0.318	3.972	0.46	0.1409	0.00375	9	0
R12P1	1.15	1.87	2	0.385	2.94	0.84	0.2991	0.003911	14	1.896
R12P2	1.15	1.87	2	0.385	3.336	0.62	0.2072	0.003911	14	0.348
R12P3	1.15	1.87	2.75	0.385	3.864	0.52	0.1615	0.003911	14	0.564
R13P1	1.15	1.87	2	0.436	3.06	0.9	0.3141	0.004177	21	2.268
R13P2	1.15	1.87	2	0.436	3.456	0.67	0.22	0.004177	21	0.492
R13P3	1.15	1.87	2.75	0.436	3.972	0.59	0.1807	0.004177	21	0.672
R14P1	1.15	1.87	2	0.487	3.048	1.27	0.4441	0.004169	19	3.024
R14P2	1.15	1.87	2	0.487	3.456	0.97	0.3185	0.004169	19	1.656
R14P3	1.15	1.87	2.75	0.487	3.936	0.81	0.2492	0.004169	19	0.708
R15H1P1	1.15	1.87	2	0.487	3.048	1.27	0.4441	0.004169	F. FLOOD	1.86
R15H1P2	1.15	1.87	2	0.487	3.456	0.97	0.3185	0.004169	F. FLOOD	1.656
R15H1P3	1.15	1.87	2.75	0.487	3.936	0.81	0.2492	0.004169	F. FLOOD	1.2
R16H4P1	1.15	1.87	2	0.487	3.048	1.27	0.4441	0.004169	DT=2.5 M	1.32
R16H4P2	1.15	1.87	2	0.487	3.456	0.97	0.3185	0.004169	DT=2.5 M	0.312
R16H4P3	1.15	1.87	2.75	0.487	3.936	0.81	0.2492	0.004169	DT=2.5 M	0.252
R17H5P1	1.15	1.87	2	0.487	3.048	1.27	0.4441	0.004169	DT=5.0 M	1.308
R17H5P2	1.15	1.87	2	0.487	3.456	0.97	0.3185	0.004169	DT=5.0 M	0.3
R17H5P3	1.15	1.87	2.75	0.487	3.936	0.81	0.2492	0.004169	DT=5.0 M	0.024
R18H6P1	1.15	1.87	2	0.487	3.048	1.27	0.4441	0.004169	DT=7.5 M	1.26

RUN #	PARTICLE ST.DEVIAT.	SED.MEAN DIAM.(D50)	PIER DIAM.(b)	Q	APPR. DEPTH(Y1)	APPR. VELOCITY	FROUD NO.	BED SLOPE	DURA-TION	MAX SCR. DEPTH(Ys)
		(mm.)	(inch)	(cfs)	(inch)	(ft/sec)			(hrs.)	(Inch)
R18H6P2	1.15	1.87	2	0.487	3.456	0.97	0.3185	0.004169	DT=7.5 M	0.3
R18H6P3	1.15	1.87	2.75	0.487	3.936	0.81	0.2492	0.004169	DT=7.5 M	0
R19H6P1	1.15	1.87	2	0.487	3.048	1.27	0.4441	0.004169	DT=15 M	1.488
R19H6P2	1.15	1.87	2	0.487	3.456	0.97	0.3185	0.004169	DT=15 M	0.252
R19H6P3	1.15	1.87	2.75	0.487	3.936	0.81	0.2492	0.004169	DT=15 M	0
R20P1	1.15	1.87	2	0.596	2.88	1.46	0.5252	0.004169	30	3.072
R20P2	1.15	1.87	2	0.596	3.492	1.13	0.3692	0.004169	30	2.592
R20P3	1.15	1.87	2.75	0.596	3.828	0.95	0.2964	0.004169	30	2.388
R21P1	2.17	1.8	2	0.385	3.36	0.695	0.2315	0.003406	17	0.492
R21P2	2.17	1.8	2	0.385	3.564	0.62	0.2005	0.003406	17	0.12
R21P3	2.17	1.8	2.75	0.385	3.828	0.49	0.1529	0.003406	17	0.264
R22P1	2.17	1.8	2	0.487	3.408	0.895	0.296	0.003406	22	0.564
R22P2	2.17	1.8	2	0.487	3.72	0.801	0.2535	0.003406	22	0.492
R22P3	2.17	1.8	2.75	0.487	3.804	0.698	0.2185	0.003406	22	0.492
R23P1	2.17	1.8	2	0.596	3.468	1.122	0.3678	0.003406	25	1.224
R23P2	2.17	1.8	2	0.596	3.552	0.981	0.3178	0.003406	25	0.792
R23P3	2.17	1.8	2.75	0.596	3.744	0.848	0.2675	0.003406	25	0.768
R24P1	2.17	1.8	2	0.731	3.48	1.346	0.4405	0.003232	24	1.884
R24P2	2.17	1.8	2	0.731	3.408	1.238	0.4094	0.003232	24	1.668
R24P3	2.17	1.8	2.75	0.731	3.648	1.135	0.3628	0.003232	24	1.812
R25H1P1	2.17	1.8	2	0.73	3.48	1.346	0.4405	0.003232	F. FLOOD	1.2
R25H1P2	2.17	1.8	2	0.73	3.408	1.238	0.4094	0.003232	F. FLOOD	1.2
R25H1P3	2.17	1.8	2.75	0.73	3.648	1.135	0.3628	0.003232	F. FLOOD	1.248
R26H4P1	2.17	1.8	2	0.73	3.48	1.346	0.4405	0.003232	DT=2.5 M	0.984
R26H4P2	2.17	1.8	2	0.73	3.408	1.238	0.4094	0.003232	DT=2.5 M	0.816
R26H4P3	2.17	1.8	2.75	0.73	3.648	1.135	0.3628	0.003232	DT=2.5 M	1.236

RUN #	PARTICLE ST.DEVIAT.	SED.MEAN DIAM.(D50) (mm.)	PIER DIAM.(b) (inch)	Q (cfs)	APPR. DEPTH(Y1) (inch)	APPR. VELOCITY (ft/sec)	FROUD NO.	BED SLOPE	DURATION (hrs.)	MAX SCR. DEPTH(Ys) (inch)
R27H5P1	2.17	1.8	2	0.73	3.48	1.346	0.4405	0.003232	DT=5.0 M	0.972
R27H5P2	2.17	1.8	2	0.73	3.408	1.238	0.4094	0.003232	DT=5.0 M	0.984
R27H5P3	2.17	1.8	2.75	0.73	3.648	1.135	0.3628	0.003232	DT=5.0 M	1.236
R28H6P1	2.17	1.8	2	0.73	3.48	1.346	0.4405	0.003232	DT=7.5 M	1.248
R28H6P2	2.17	1.8	2	0.73	3.408	1.238	0.4094	0.003232	DT=7.5 M	1.368
R28H6P3	2.17	1.8	2.75	0.73	3.648	1.135	0.3628	0.003232	DT=7.5 M	1.248
R29P1	1.28	0.76	2	0.267	3	0.585	0.2062		8	0.624
R29P2	1.28	0.76	2	0.267	3.468	0.44	0.1442		8	0.12
R29P3	1.28	0.76	2.75	0.267	3.864	0.4	0.1242		8	0.06
R30P1	1.28	0.76	2	0.344	2.976	0.761	0.2693		20	2.424
R30P2	1.28	0.76	2	0.344	3.372	0.558	0.1855		20	0.96
R30P3	1.28	0.76	2.75	0.344	3.768	0.5	0.1572		20	0.672
R31P1	1.28	0.76	2	0.422	3.12	0.855	0.2955		21	3.204
R31P2	1.28	0.76	2	0.422	3.564	0.628	0.2031		21	2.292
R31P3	1.28	0.76	2.75	0.422	3.96	0.572	0.1755		21	1.86
R32P1	1.28	0.76	2	0.487	3.12	0.979	0.3384		23	3.336
R32P2	1.28	0.76	2	0.487	3.564	0.836	0.2703		23	2.604
R32P3	1.28	0.76	2.75	0.487	3.96	0.671	0.2058		23	3.276
R33H4P1	1.28	0.76	2	0.487	3.12	0.979	0.3384		DT=2.5 M	1.848
R33H4P2	1.28	0.76	2	0.487	3.564	0.836	0.2703		DT=2.5 M	1.548
R33H4P3	1.28	0.76	2.75	0.487	3.96	0.671	0.2058		DT=2.5 M	0.9
R34H5P1	1.28	0.76	2	0.487	3.12	0.979	0.3384		DT=5.0 M	2.136
R34H5P2	1.28	0.76	2	0.487	3.564	0.836	0.2703		DT=5.0 M	1.836
R34H5P3	1.28	0.76	2.75	0.487	3.96	0.671	0.2058		DT=5.0 M	0.948
R35H1P1	1.28	0.76	2	0.487	3.12	0.979	0.3384		F. FLOOD	2.028
R35H1P2	1.28	0.76	2	0.487	3.564	0.836	0.2703		F. FLOOD	1.98

RUN #	PARTICLE ST. DEVIAT.	SED. MEAN DIAM. (D50) (mm.)	PIER DIAM. (b) (inch)	Q (cfs)	APPR. DEPTH (Y1) (inch)	APPR. VELOCITY (ft/sec)	FROUD NO.	BED SLOPE	DURATION (hrs.)	MAX SCR. DEPTH (Ys) (inch)
R35H1P3	1.28	0.76	2.75	0.487	3.96	0.671	0.2058		F. FLOOD	1.656

